UNIVERSITÀ DI PARMA

UNIVERSITA' DEGLI STUDI DI PARMA

DOTTORATO DI RICERCA IN

"Scienze Mediche e Chirurgiche Traslazionali"

CICLO XXXIV

CARDIOMYOCYTES CONTRACTION *IN VITRO* CHARACTERIZATION: NEW VIDEO-KINETIC APPROACH

Coordinatore:

Chiar.mo Prof. Nicola Sverzellati

Tutore:

Chiar.mo Prof. Michele Miragoli

Dottorando: Amparo Guerrero Gerbolés

Anni Accademici 2018/2019 – 2020/2021

Summary

ABSTRACT

Cardiovascular diseases impact on the global population continues to increase, and as the understanding of the plethora of phenomena involved in cardiac disease phenotypes advances, *in vitro* models predictivity reaches a plateau. The development of new models that resemble more faithfully *in vivo* pathophysiological conditions inevitably faces the lack of versatile functional evaluations capable of analysing different sample configurations without destructing them.

Over the past years, in particular, the importance of characterizing cardiac contractile profile became clear; elucidating cardiomyocytes contraction patterns in a controlled environment, indeed, facilitates the understanding of genetic variations functional implications and cardiovascular diseases progression.

In this work, human pluripotent stem cells were differentiated in cardiomyocytes and cultured as beating monolayers. The contractile behaviour of this cell culture was studied through video microscopy with a new software for movement quantification, and a dedicated algorithm for signal analysis.

This analytical set succeeded in detecting a decrease in contractile activity in later stages of cardiomyocytes differentiation and proved to be sensitive to contraction variations following Isoproterenol treatment. Additionally, it provided interesting insights into distanced cardiomyocytes mechanical synchronization.

1. INTRODUCTION

1.1 CARDIOVASCULAR DISEASES

Cardiovascular diseases (CVDs) remain the primary cause of death in the world. This group of multifactorial disorders impact both on heart and blood vessels and include a wide range of pathologies such as ischemic heart disease, myocardial infarction (MI), stroke, peripheral arterial disease, deep vein thrombosis and pulmonary embolism, and congenital heart diseases (CHDs), together with other cardiac and vascular conditions. [1,2]

In addition to these diseases, several non-cardiac therapies determine adverse reactions that cause similar disease phenotype or aggravate pre-existing disorders and are generally referred as determining cardiotoxic.[3,4] Cardiotoxicity can affect both cardiomyocytes structure and electrophysiology; the first is the case of most drugs designed to be cytotoxic, such as chemotherapeutic agents, that determine an increase in oxidative stress, mitochondrial damage and apoptosis; [4–7] the second form of cardiotoxicity, instead, impairs cardiomyocytes' electrical homeostasis by affecting heart frequency and/or the action potential shape.[4]

All these different conditions, determined by genetic, environmental or therapeutic factors, eventually determine an alteration of cardiac contraction, reduction in its ejection fraction, arrhythmias, pathological myocardial remodelling -through excessive extracellular matrix (ECM) deposition and cardiomyocyte hypertrophy-, and heart failure (HF).[8]

Current pharmacological therapies are mainly palliative and target patients with an advanced stage of pathology when irreversible remodelling has already occurred [9], as a result of the difficulties in understanding the functional implications of the extensive knowledge acquired so far on genetic variants associated with cardiomyopathies and CVDs in general. [10] Indeed, the technological advance of the past decades and the possibility of performing genomic studies on large expression datasets, facilitated the identification of causal genes for several CVDs, and in particular for CHDs.[8] Nevertheless, it is still challenging to link mutation-induced molecular insults with the pathological phenotype: during the pathogenic cardiac remodelling different compensatory and maladaptive pathways are activated, introducing a wide variability that prevents a straight correlation between mutations and phenotypic expression.[11]

Given these considerations, linking genetic mutations with disease phenotype is still a primary challenge in clinical medicine and basic science.

1.2 *IN VITRO* MODELS FOR CARDIOVASCULAR DISEASE

As previously stated, advances in cardiovascular research have highlighted the complexity of CVDs and their classification, both in terms of molecular aetiology and clinical phenotype.

Genomic investigations provided a significant boost to cardiovascular disease understanding, but a further elucidation of its mechanisms requires functional assessments through *in vitro* modulation of cell cultures or/and *in vivo* animal models, to validate the biological relevance of identified genetic variants.[8] In the case of CHDs, in particular, the identification of the functional implications of the early molecular response would enable to target either the primary biophysical defect or the initial downstream signalling pathway, thus potentially changing the progression of the pathological cardiac remodelling.[12]

Cardiovascular research has long relied on animal models to study cardiac physiology and pathophysiology, for they recapitulate human cardiac physiology with good approximation. [4] Initial applications of animal models concerned the development and testing of surgical procedures and pharmacological treatments *in vivo*,[13] and were rapidly followed by the development of intact muscle preparation for *ex vivo* manipulation and investigation.[14] However, as the focus of the research shifted from macroscopic observations to more detailed functional examinations, the whole organ and isolated muscle preparations revealed several limitations: not only do they prevent analysis of the middle of the muscle, and limit the use of imaging techniques, but the large size of the samples also impede a proper control of membrane potential during electrophysiological assessments; thus determining the emergence of models based on isolated cardiomyocytes and cell lines to better understand the cellular and subcellular physiology and pathophysiology.[15]

At present, cell cultures remain a relevant model in cardiovascular research; nonetheless, the translation remains challenging considering the poor sequence conservation of non-coding sequences across species [8] and the difficulty of replicating human heart conditions *in vitro*. [16]

Mimicking organ conditions, indeed, is of particular importance in cell cultures in general and in cardiomyocyte cultures in particular. Culture conditions greatly impact cell morphology, and in the case of cardiomyocytes morphology is strictly related to function; it has been reported that morphology impacts electrical properties in atrial myocytes, and the size-dependent variance in ionic currents may be related to the electrical activity differences in the various cardiac areas. [17,18]

This evidence has led, over the past years, to an increasing effort to develop new *in vitro* models with enhanced complexity that can recapitulate the variability of clinical expression not only from a molecular point of view but also from a biophysical perspective. These models are progressively supporting investigations based on traditional cell cultures, that remain the most versatile, economic, and convenient model. [16]

1.2.1 PRIMARY CARDIOMYOCYTES

Primary cardiomyocytes obtained from small rodents represented one of the first and invaluable models to study cellular and subcellular physiology through electrophysiology, calcium imaging, cell mechanics, immunohistochemistry and protein biochemistry.[15] Certainly, isolation of human cardiomyocytes from surgical waste is also a practicable procedure, however, the low availability of samples, the low yields of obtained cardiomyocytes and the risk of de-differentiation in extended cultures, together with ethical and logistic problems related to human tissue usage, makes impractical to employ human primary cardiomyocytes in most of the cases.[4,16,19]

Adult primary cardiomyocytes

Methods for cardiomyocyte isolation were developed nearly 50 years ago[20], nevertheless, there is no universal protocol that ensures a large yield of viable cells, leading to several variations to better fit the purpose and application of each research group.[15]

Animal-derived cardiomyocytes are mainly obtained by the Langendorff method, performing perfusion of enzyme solutions through the aorta of an isolated heart using either constant pressure or constant flow,[21] although some groups succeeded in isolating CMs by mincing and agitating the left ventricle of small animals in dishes containing the enzymatic solution. [22]

Digestion of rat or mouse hearts relies on proteolytic enzymes, primarily including collagenases (type II and IV), and proteases (type XIV), but also pancreatin and trypsin,[18,23,24] and is preceded by the perfusion of a low calcium solution to disrupt the intercellular connections at the intercalated discs. [25]

Although freshly isolated CMs are considered more physiologically relevant in terms of both structure and function, together with the setup of isolation protocols great effort was also put into the development of cultures of primary adult cardiomyocytes, with the intent of maintaining a homogenous population of cells over longer periods, thus allowing extended treatments and analysis. [15]

It was soon assessed that rapidly promoting cell attachment through serum-free medium and coating of the culturing substrate, resulted in better preservation of morphology compared to prolonged suspension cultures; [26] this approach relies on several options for the substrate coating, including Laminin, Fibronectin, or synthetic peptides, [27,28] whereas for the culture medium, a basic medium is commonly supplemented with creatine, carnitine and taurine, with particular attention to buffering and ionic composition. [29] Adult cardiomyocytes cultured in adhesion were reported to remain quiescent and viable for 2 weeks,[29] however within the first week there's a significant loss of cells (about 50-70%) and both morphological and functional changes: cells shorten, lose definition in their striation, t-tubule density reduces, the resting membrane potential decreases as well as the K+ current

density, action potential lengthens, and L-type calcium current peak decreases. [30–32] Different strategies were studied to delay these modifications, such as electrical pacing and treatment with adrenergic agonist, [33,34] but failed to completely inhibit or reverse cell adaptation to culturing conditions and determined, in the case of adrenergic agonists, also the activation of hypertrophic and apoptotic pathways. [33] As a result, studies involving primary adult cardiomyocytes require shorter cultures and particular attention to control experimental conditions in order to obtain relevant data.

Neonatal primary cardiomyocytes

In alternative to adult cardiomyocytes, it is also possible to isolate neonatal cardiomyocytes from 1-5 days old mice or rats, although most of the protocols present in the literature concern neonatal rats. These cells not only are more easily kept in culture and display spontaneous beating activity, but also require a simpler isolation procedure compared to adult CMs since enzymatic digestion and mechanical agitation are enough to obtain the cardiomyocytes, and aorta cannulation and perfusion are not performed;[35] furthermore, the simultaneous digestion of multiple hearts (a rat litter typically consist of 10-20 pups) allows to increase the yield of cardiomyocytes. [15] Over the past decades, several protocols for murine neonatal cardiomyocyte isolation have been proposed, although the backbone of the procedure remains unaltered. The procedures involve the heart excision within the 5th day of pup's life, followed by the steps of washing, mechanical dicing and enzymatic digestion by gentle stirring; the preferred enzymes to perform the single-cell dissociation are trypsin, collagenase and pancreatin, either on their own or in combination. [36]

Neonatal rat cardiomyocytes were extensively employed to study morphological, molecular and electrophysiological changes to drug delivery and toxicity, [37] hypoxia and reoxygenation scenarios,[38,39] and pathological phenomena such as apoptosis, necrosis and autophagy.[40]

Nevertheless, this cell population displays subcellular organization and morphological differences compared to adult cardiomyocytes; indeed, neonatal cardiomyocytes derived from small rodents present immature t-tubular subsystem, disorganized contractile machinery distribution, and may employ different components in common signalling pathways. These findings disclose the difficulty in a proper translation of findings concerning ionic-fluxes studies and excitation-contraction coupling.[36]

1.2.2 CARDIOMYOCYTES CELL LINES

As already reported in the studies that rely on primary cardiomyocytes, there's a limited temporal window to perform experiments when working with isolated CMs; indeed, terminally differentiated primary cultures can be maintained for nearly 14 days but rapidly undergo morphological and functional changes over time; [41] furthermore, the intra- and inter-experimental heterogeneity of the obtained cell populations often undermine experimental findings and their reproducibility.[42]

These observations lead research efforts to develop stabilized cardiomyocytes cell lines.

HL1 cell line

HL1 represented a milestone in the development of cardiomyocyte cell lines. Previous attempts to develop a proliferating line of cardiomyocytes had led to cell lines that gradually lost either their cardiac phenotype or the proliferative activity over continuous passages. [43]

HL1 cells were obtained from AT1 cells. These highly differentiated cardiomyocytes derived from an atrial tumour of a transgenic mouse, in which SV40 expression was targeted to atrial cardiomyocytes through ANF promoter; [44] nevertheless one of the biggest pitfalls concerned their maintenance, that required the serial propagation as ectopic grafts in syngeneic mice, since AT1 cells could not be passaged nor recovered from frozen stocks. Through culturing AT1 cells in selective conditions, Claycomb and colleagues succeeded in creating a cell line of atrial cardiomyocytes that not only can be serially passaged and recover from frozen stocks, but also maintains both its differentiated phenotype and contractile activity; the main variations in the culturing conditions consisted in using Ex-Cell 320 medium with the addition of endothelial cell growth supplement to promote cell division, and retinoic acid and norepinephrine to stimulate beating activity and maintain the differentiated phenotype. [43]

These conditions led to the selection of cells with several characteristics of adult cardiomyocytes: similar ultrastructure, highly ordered myofibrils and cardiac-specific junctions organized in the intercalated disc, distinctive pattern of gene expression (alfa- myosin heavy chain, alfa-cardiac actin, desmin, connexin-43), and several characteristic voltage-dependent currents, in particular Ikr. In addition, HL1 display the ability to undergo spontaneous contractions, which makes them particularly appealing for studies that require an adult-specific phenotype and for performing functional analysis. [43,45]

AC16 cell line

Davidson and his team. succeeded in establishing a proliferating human cardiomyocyte cell line by fusing primary human ventricular cardiomyocytes with SV40 transformed, uridine auxotroph human fibroblasts, deprived of mitochondrial DNA. Following the selection of successfully fused cells, the group identified a promising clone, AC16, that was morphologically uniform and expressed several cardiomyocyte markers such as transcription factors (GATA4, MYCD and NFATc4), contractile proteins (α- and β- myosin heavy chain, α-cardiac actin, troponin I) and functional gap junction proteins (connexin-43 and connexin-40). However, further findings suggest that the AC phenotype is pre-contractile and de-differentiated. Indeed, the transformation by the SV40 gene, which induces the cardiomyocytes to re-enter the cell cycle, may also prevent the complete expression of

cardiomyocyte phenotype: not only do AC16 cells lack organized sarcomeres and T-tubules, but they also display a low resting potential and an absence voltage-activated conductances. [42]

The resulting model, has the merit of being a human cell line and results particularly useful in the study of signalling pathways that regulate cardiomyogenesis, and to evaluate pharmacological and physiological effects of drugs on a molecular basis;[46,47] but may fail when functional analysis on cardiomyocytes' activity is required (either electrophysiology analysis or contraction evaluation).

1.2.3 hPSC DERIVED CARDIOMYOCYTES

The advent and progress in human pluripotent stem cell (hPSC) derivation, culture and differentiation, provided an alternative and promising source of cardiomyocytes for cardiac cell biology investigation, drug development and cardiac therapeutics studies, proving particularly predictive in the early stages of preclinical research; [4,48,49] Several differentiation strategies (from pluripotent stem cells to cardiomyocytes) have been progressively developed [50] and, currently, complete kits for cardiomyocyte differentiation are commercially available, as chemically defined media supplemented with growth factors or small molecules that activate specific pathways.[51–53]

This standardization of pluripotent stem cells culture and differentiation, together with the growing diffusion of dedicated cell banks for both healthy and diseased hPSCs, significantly encouraged the use of hPSC derived cardiomyocytes (hPSC-CMs) and laid the foundation for their characterization as potential cardiovascular models. [4]

As for neonatal cardiomyocytes, the main drawback of this model lies in is its phenotypic immaturity. Morphologically, these cardiomyocytes display round and small shape, disorganized contractile machinery;[54] furthermore, they also exhibit a depolarized membrane potential that together with a lower expression of ionic channels and the presence of funny currents, leads to spontaneous contractions;[55,56] the diversity in channel numerosity also determines a slower electrical propagation, and variations in the calcium handling (mainly attributable to a decreased expression of calsequestrin, ryanodine receptor type 2, and phospholamban) implies a delayed excitation-contraction coupling. [56,57] Nevertheless, great effort has focused over the past years on hPSC-CMs maturation and several strategies have been proposed: from defined culture conditions to exogenous stimuli including electrical pacing, substrate stiffness, 3D cultures, and heterotypic co-cultures; [58–62] through this approach an increase in ion channel expression and consequently an improvement of the functional properties were reported. [4] Furthermore, several studies consistently highlighted hPSCs-CMs effectiveness in modelling cardiovascular genetic disease phenotypes,[63–65] predicting cardiotoxicity,[66,67] testing novel drugs or personalized therapeutic approaches.[68,69]

Hence, despite their phenotypical immaturity implies a particular caution when translating results to more complex models, hPSC-CMs have progressively been established as a valuable cell source in

cardiovascular research, by modelling myocardial pathophysiology *in vitro*. Compared with primary cardiomyocytes hPSC-CMs can be conveniently cultured for longer periods and, despite their morphological immaturity, better resemble the sarcomeric contractile machinery that is known to be different between human and rodent cardiomyocytes. [70] In addition, compared to the use of human immortalized cell lines, the possibility of deriving hPSCs-CMs from patients and potentially creating syngenic control lines significantly increases the model relevance and represents a considerable breakthrough in the study of pathological phenotypes, disease mechanisms and pharmacological response, that benefit from studies on disease-specific samples.

1.5 *IN VITRO* FUNCTIONAL ASSESSMENTS FOR CARDIOMYOCYTES CULTURES

A pivotal aspect that requires a detailed study is the assessment of the biophysical performance of *in vitro* cardiovascular models. Indeed, in the clinical context, symptoms and outcomes of cardiovascular diseases are mainly defined by the functional alterations detected on myocardial performance.[12] From this perspective, the possibility of studying the link between mutation or drug interference and functional disruption *in vitro* provides valuable insights into pathological phenotype classification and cardiotoxicity mechanisms.

1.5.1 STANDARD FUNCTIONAL CHARACTERIZATION

At present, most of CMs functional characterization relies on studying the electrophysiological behavior, and studies on the signalling and handling of calcium.

In vitro electrophysiological assessments are quantified either through patch-clamp or microelectrode arrays (MEAs). [71]

The patch-clamp technique allows the recording of single/small groups of ion channels, intracellular membrane potentials and currents in varied biological substrates, from isolated primary cells and cell lines to isolated tissue sections and even *in vivo* models. This technique relies on the use of micropipettes to create a high resistance seal on reduced portions of the cell membrane, thus allowing the recording of single or small groups of ion channels, with a significant increase of the signal/noise ratio.[72] Several configurations are described and optimized according to the experimental requirements: (i) cell-attached, to study single ion channels in a small portion of cell membrane, (ii) loose-seal cell-attached, to investigate a wider area of the membrane and record isolated action potentials of single cells, (iii) inside-/outside-out, that ensures the recording of single ion channels from the intra- or extracellular portion isolated from the rest of the cell, (iv) whole cell, to record currents and action potentials, (v) perforated patch, to decrease the cell dialysing rate of the previous configuration, by introducing small pores to the membrane through antifungal/antibiotic agents; and two recording modes are possible: (i) Current-clamp, that applies a constant current and records the

membrane potential over time and/or following external stimuli such as pharmacological intervention; (ii) Voltage-clamp, that sets a controlled potential in the membrane and records the required current to maintain that voltage, and is particularly useful to characterize single ion channel properties. [73]

Alternatively, electrical activity can be evaluated non-invasively with MEAs. This technology consists of a set of organized electrodes placed on the surface of a culturing chamber. Electrodes not only allow local stimulation but also the simultaneous recording of extracellular potentials in multiple sites with a high spatiotemporal resolution; as a result, this technique is often used to study interactions among electrogenic cells, study the spatiotemporal dynamics of the electrical activity of a tissue or cell population, and to efficiently sample the electrophysiological behaviour of larger areas. [74]

Along with the patch-clam technique, calcium transients can be studied through optical imaging using either fluorescent cation-sensitive synthetic molecules or genetically encoded calcium indicators; however, the technical difficulties of introducing into genetically encoded indicators in the desired models, their limited dynamic range and their reduced kinetics determined the emergence of chemical indicators as a method of choice, and currently, a wide range of Ca2+ sensitive dyes are commercially available. These calcium indicators can be classified into two main groups: (i) single wavelength indicators, that vary their fluorescence intensity according to calcium concentration, and (ii) double-wavelength indicators, that undergo a shift in their excitation or emission wavelength. [75]

1.5.2 CARDIOMYOCYTES CONTRACTION EVALUATION

The abovementioned techniques (patch-clamp, MEAs, calcium reporters) belong to a long tradition of established technologies aimed to quantify electric and calcium,[76] and proved to be comparable across different laboratories, cardiomyocyte sources and culturing methods. [77,78]

Nevertheless, over the past years, the need for an appropriate platform for contraction assessment in multiple sample conditions (from single cells and monolayers to isolated tissue and organ) has progressively emerged. Indeed, despite being a salient feature of cardiomyocytes' function, contraction evaluation is frequently missing in cardiomyocytes characterization; more systematic contraction evaluation holds great potential not only in the study of genotype-phenotype correlation in new disease models derived from patient hPSCs but also in the characterization of disease progression and drug cardiotoxicity. [62,63,79,80] Among the reasons for this gap, certainly the specificity of the available techniques for specific cell configurations plays an important role.

Following, a brief description of the main techniques for contraction assessment is provided.

Cell Traction Force Microscopy (CTFM)

This technology allows estimating cell's traction force based on their ability to deform a substrate. Over the years the technique evolved from the macroscopic evaluation of the diameter contraction of a collagen disk to the development of micropatterned substrate of polyacrylamide embedded with fluorescent beads. The deformation of the substrate with known elastic modulus is recorded through the variations of fluorescent beads positions, and the traction force can be obtained through the application of the elasticity theory. [81]

Despite the elegance of the approach, this strategy requires a careful selection of the substrate properties and control of the experimental conditions and can fail to properly detect low contractile forces.

Label-free video microscopy

This technology, relying on high-speed video microscopy, has quickly overtaken traction force microscopy, partially due to the simplicity and availability of the instrumental setup.[82–84] Furthermore the non-invasiveness of the analysis allows the preservation of the sample integrity and sterility, facilitating long-term monitoring of its contractile parameters.

This approach includes different techniques that differ by the tracking strategy employed to quantify the substrate movement.

One of the first strategies developed was Edge Detection. This technology takes advantage of the strong border information of adult cardiomyocytes in bright-field with a smooth background; changes in the position of this feature (the border) can be, therefore, easily tracked and quantified by dedicated algorithms, such as the Canny operator.[85] One of the main values of edge detection and its derivatives, such as sarcomere and perimeter detection, relies on providing measurements in standard units that facilitate data interpretation and avoids relative quantification; however, the specific nature of the tracking strategy significantly limits its application to few cell sources and culturing conditions and is prone to introduce errors when cell geometry and torquing deviate from standard behaviour. [86] So far, edge detection has proved particularly suitable for adult single cardiomyocytes [84] and isolated hESC-CMs embryonic bodies [87]

In response to the limits of feature-based tracking, which requires the precise and conserved identification of a moving element, other research groups shifted their focus on pixel variations. Hayakawa and co-workers, for example, averaged the displacement vectors of a cardiomyocytes monolayer to characterize its beating pattern, with a technique defined optical flow; displacement vectors were identified by dividing the acquired image into multiple sections and exploiting the section's pixel distribution profile as a marker to identify their position in the following frames; their findings also suggested that this average value obtained correlates to the force exerted by the

cardiomyocyte. [88] Mummery's group, instead, further simplified the approach by considering the percentage of pixel intensity variation through time as an approximation of the field movement and correlating the profile thus obtained both with optical flow analysis and sarcomere shortening analysis. [71,89]

These investigations, performed independently by different research groups, confirmed that variations on cardiomyocytes electrophysiology and function impacts contractile motion, and gave evidence that contraction can be efficiently quantified by high-speed video recordings.

1.8 AIM OF THE WORK

In the present work, a new software (LOKI) for automated cardiomyocytes movement quantification is proposed, supported by a dedicated algorithm that characterizes the contraction profile. The software analyses video recordings, applying an automatic threshold to the image and quantifying the percentage of moving pixels for each frame, in relation to a reference frame.

The versatility and sensitivity of this analytical set were applied to characterize differentiating hPSC-CMs monolayers mechanical behaviour.

In particular, the technology was employed to study (i) the variations in cardiomyocytes contraction at different time points, (ii) their response to a chronotropic and inotropic agent, and (iii) the mechanical synchronization of distanced regions of a given beating field.

2. MATERIALS AND METHODS

2.1 HUMAN PLURIPOTENT STEM CELL CULTURE AND EXPANSION

Commercially available human pluripotent stem cells (hPSCs) were donated by Humanitas Research Hospital (Dr, Elisa di Pasquale's group).

hPSCs were expanded with Essential8 Medium (cat. A1517001, Thermo Fisher) on 6-wells plates (cat. 3516, Corning) coated with Corning® Matrigel® Growth Factor Reduced (GFR) Basement Membrane Matrix at a final concentration of 0,08mg/ml.

Once a week, cells were passaged; hPSCs were incubated with EDTA 0,5uM (cat. AM9260G, Thermo Fisher) for 3' at 37°C and were following detached by pipetting fresh medium on the well's surface. The cell suspension was centrifuged at 300g and the obtained pellet was seeded, at the required cell density, on a new coated plate with the addition of 1uM of rock inhibitor (cat. S1049, Selleckhem). to the culturing medium. During cellular expansion medium was daily changed.

2.2 hPSC DIFFERENTIATION INTO CARDIOMYOCYTES

hPSC were differentiated into cardiomyocytes following the indications of the Gibco® PSC Cardiomyocyte Differentiation Kit (cat. A2921201, Thermo Fisher). The kit consists of three chemically defined media (A, B and M) and is based on the work of Burridge; [53] therefore, the key mechanism is an initial stimulation of the Wnt pathway and a successive inhibition of it.

Briefly, hPSC were expanded, as previously described, until they reached a confluency of 70%; on the first day of the differentiation protocol, Essential 8 Medium was replaced with Cardiomyocyte Differentiation Medium A; no further medium change was performed until day 3, when the medium was replaced with Cardiomyocyte Differentiation Medium B; following, cells were kept in the same medium for further two days, and on the 5th day of differentiation, it was replaced with Cardiomyocyte Maintenance Medium M. Maintenance medium was changed every two days and cells were cultured for an average of 25-30 days.

2.3 CARDIOMYOCYTES PURIFICATION

After 25-30 days of differentiation, cells were enzymatically dissociated with a Multi Tissue Dissociation Kit (cat. 130-110-201 MACS Miltenyi Biotec) and filtered with 70µm strainers. Cells thus obtained were enriched for cardiomyocytes through an indirect labelling and magnetic separation of non-cardiomyocytes with the PSC-Derived Cardiomyocyte Isolation Kit Human (cat. 130-110-188 MACS Miltenyi Biotec): briefly, cells were resuspended in a Non-Cardiomyocyte Depletion Cocktail and later labelled with Anti-Biotin MicroBeads; the cell

suspension was then applied to the LS Columns to perform the magnetic separation and the non-labelled cells (hPSC-derived CMs) that passed through the column were collected and seeded on coverslips coated with Matrigel at a cell density of 5x105 cells/well. Cells were kept in culture in DMEM High Glucose (cat. L0101, Thermo Fisher) with the addition of Non-Essential Amino Acids (cat. BE13-144E, Lonza), 2%FBS (cat. 12103C, Sigma), 100 U/mL Penicillin, 0,1mg/mL Streptomycin and 50µM β-mercaptoethanol.

2.4 CARDIOMYOCYTES CHARACTERIZATION

Cells dedicated to immunofluorescence assays were fixated with 4%PFA and permeabilized with Triton 0,1%. Aspecific binding sites were saturated with Goat Serum 5%. Primary antibodies, mouse monoclonal Anti-α-Actinin (Sarcomeric) (cat. A7732, Sigma) and rabbit Anti-Troponin I (ab47003, Abcam), were both diluted 1:250 in Goat Serum 2% and incubated O.N. at 4°C in a humidified chamber. Secondary antibodies, Goat anti-Mouse Alexa Fluor 555 (cat. A28180, Thermo Fisher) and Goat anti-Rabbit Alexa Fluor 488 (cat. A27034, Thermo Fisher), were diluted 1:1000 in Goat Serum 2% and incubated 1h at 37°C in a humidified chamber. Nuclei were stained with NucBlue™ Fixed Cell ReadyProbes™ Reagent (cat. R37605, Thermo Fisher), 2 drops/ml in PBS.

2.5 ISOPROTERENOL TREATMENT

Before the purification step, beating monolayers of differentiating hPSCs were treated with 1uM Isoproterenol (xxx, Sigma). The stock solution was prepared in PBS at the concentration of 1mM and directly diluted in the cells' medium at the time of the treatment.

Treatment was performed at different time points of the differentiation process (D14, 21, 28 and 35). And cell response was assessed 5'-30' after diluting the Isoproterenol in the culturing medium.

2.6 VIDEO-BASED ANALYSIS OF CONTRACTION

Beating monolayers performance was evaluated at different time points and treatment conditions, through a custom-made acquisition software and a dedicated algorithm for the output analysis (For Guide Users Interface see Figures 1S-5S on the Appendix). During the acquisitions, cells were kept in a controlled environment, at 37°C and % CO_2. Experiments were conducted in triplicate; at least 5 fields were acquired for each condition and 3-6 ROIs were analysed for each field.

Video Acquisition

5s video recordings of different fields were acquired at 140 fps with a high-speed video camera (Basler ac1920-155) mounted on an inverted microscope (Eclipse Ti2, Nikon). Acquisition and camera settings were controlled via custom-made software developed on LabVIEW. Data was saved

as a frame sequence of TIFF images, supported by a metadata file with the annotations of the recording settings.

Video Post-Processing

Acquired videos were processed with dedicated software implemented on the LabVIEW platform to obtain the beating profile of the analysed sample.

After loading the required file, the whole video was visually inspected to identify a reference frame; this reference frame was selected during the relaxation phase, between two consecutive beats. Following, the original image was modified by applying an automatic threshold: pixels with a value within the range $Mean_{pixel\ value} \pm Standard\ Deviation$ were given a value of 1, whereas the remaining pixels were conferred a value of 0. Once the threshold was established the software automatically subtracts the reference frame to every frame composing the 5s video. The output is a plot with time on the x-axis and the percentage of pixels that changed their value (from 0 to 1 and vice versa) out of the total number of pixels of the analysed region of interest (ROI)

Output analysis

The plot obtained in the post-processing stage was exported as a two-columns .txt file and analysed through a dedicated algorithm implemented in Matlab programming language.

From the dataset, the plot is recreated, and the operator identifies the starting point, peak and end-point of each recorded beat. Based on this input, the algorithm calculates the parameters of frequency, beat duration, the maximum percentage of moving pixels, time to 10-50-90% of the curve (both during contraction and relaxation), and slew rate, intended as the ratio between the percentage of moving pixels of the 10-90% section and the time required to complete that section.

2.7 STATISTICAL ANALYSIS

Data collected were analysed using the software GraphPad Prism 6. Data distribution was assessed through the Kolmogorov-Smirnov test. Normally distributed datasets were analysed with One-way ANOVA (multiple comparisons), whereas Kruskal-Wallis tests were performed on data that did not display normal distribution. Data are expressed as Mean ± SD.

3. RESULTS

3.1 hPSC-CMs DIFFERENTIATION AND CHARACTERIZATION

The initial differentiation experiments focused on the determination of the relative cell confluency at the protocol onset. With this intent, several conditions were tested, including splitting the cells as colonies or single cells at different split-ratios (1:15, 1:6) or cell densities (4,5x104, 5x104, 5,5x104, 6x104, 7x104 and 1x105 cells/well). For most of the experimental conditions, however, it was possible to perform just one purification out of at least three differentiations; the most replicable conditions were:

- Passaging the cells in colonies at 1:15 ratio and starting the differentiation after 4 days.
- Seeding the cells at a density of 50000 cells/well and starting the differentiation after 4 days.

In both conditions beating areas were observed, but the density was greater when cells were seeded at 50000 cells/well; moreover, the distribution of these areas was better spread compared to cells passaged 1:15, where clusters and networks tended to concentrate in the edges of the well.

Furthermore, seeding the cells at a cell density ranging from $5x10^5$- $5,5x10^5$ and starting the differentiation protocol after 4 days increased the differentiation efficiency, compared to the 1:15 split condition (Figure 1).

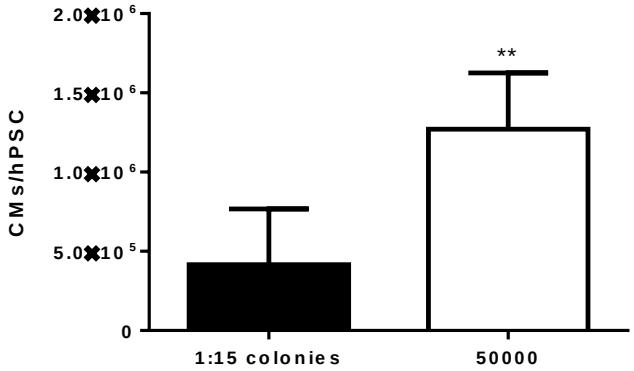

Figure 1. *Differentiation efficiency of two seeding densities. **p<0.01*

Cells obtained from the differentiation protocol were kept in culture for at least 40 days and characterized by immunofluorescence assay. Samples were tested for α-actinin and cardiac troponin I, showing positive signals for both cardiac markers (Figure 2)

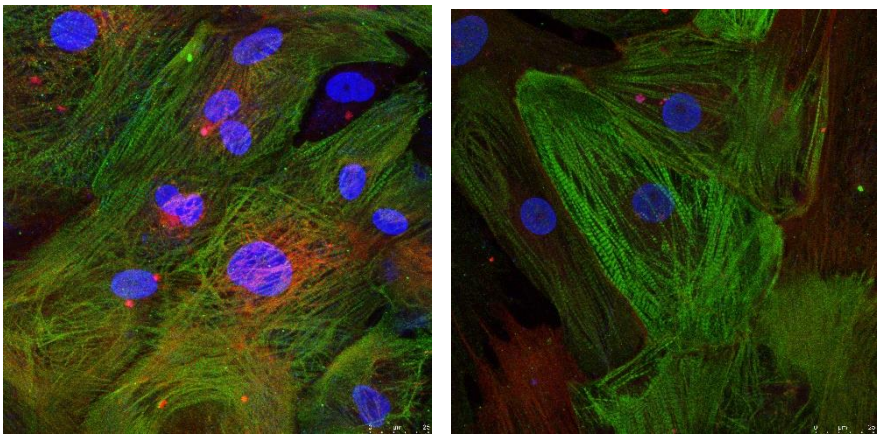

Figure 2 *Representative images from the immunofluorescence characterization of hPSC-CMs. Blue signal corresponds to DAPI, green signal stands for Troponin I and red signal corresponds to α-actinin. Scale bar: 25µm*

3.2 hPSCs CONTRACTION ASSESSMENT

hPSC-CMs were kept in culture for 5 weeks and their spontaneous contractile performance was assessed weekly after they started their beating activity. To characterize their contraction profile, the parameters of frequency, beat duration, the maximum percentage of moving pixels in contraction and relaxation, and the slew rate both in contraction and relaxation were considered.

3.2.1 Development of customized new software for kinematic analysis (LOKI)

To analyse cellular contractile performance, a brand-new software denominated LOKI (Longitudinal optokinetic incubation) was developed in LabView Environment to analyse the kinetics of beating cells from sequences of images was developed. Thanks to a collaboration with the Department of Engineers and Architecture from the University of Parma a computer vision technology was implemented to control a high-speed video camera mounted on a Nikon inverted epifluorescent microscope Ts2-Fl placed within a cell incubator (Figure 3); the setup thus organized allowed the acquisition of longitudinal mechanical data over time without interfering with hiPSC differentiation.

Figure 3. *Strumental setup, consisting on an inverted epifluorescent microscope connected with a high-speed camera (160 fps) placed within an environment with controlled temperature and CO2 concentration.*

The software applies image segmentation, a branch of image processing that focuses on partitioning an image into sections based on their characteristics and properties; different strategies and algorithms can be applied to group and split pixels, according to common characteristics, that will allow the identification of an Image Object from the rest of the image, e.g. the Background. In this specific case, the developed software adopts the threshold method as the simplest method for image segmentation. It compares the pixel's intensity with a pre-set value, the threshold, and assigns to each pixel a new value (either 0 or 1) depending on whether the original value is comprised within the threshold or not; the original greyscale image is therefore converted into a binary image (Figure 4).

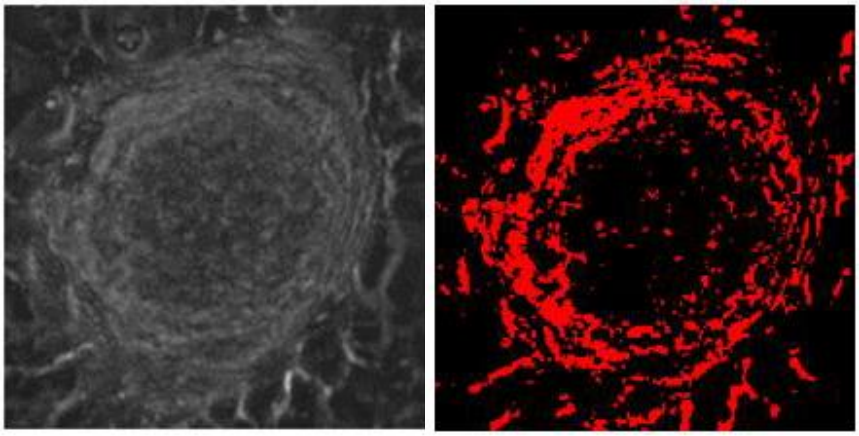

Figure 4. *Example of treshold application. On the left the original greyscale image and on the right the binary image.*

To reduce user dependency when defining the threshold value, the software was provided with an automatic threshold selection based on the central limit theorem. The main implication of this theorem is that a high percentage of the objects under study (in this case pixels in correspondence of cells) are included in the range described by the mean ± standard deviation as exemplified in Figure 5.

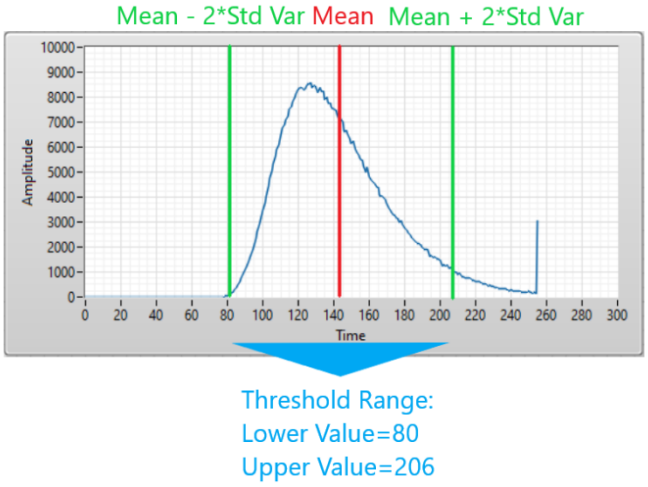

Figure 5. *Example of pixel intensity distribution and consequent threshold application.*

The software was also provided with ROI (Region of Interest) selection tools. In digital image processing, indeed, ROIs are frequently used to limit the processing and/or analysis calculations just to defined areas of an image, thus increasing the performance of the software, and decreasing noise The user can choose between four different geometries: line, circle, rectangle or manual. (Figure 6).

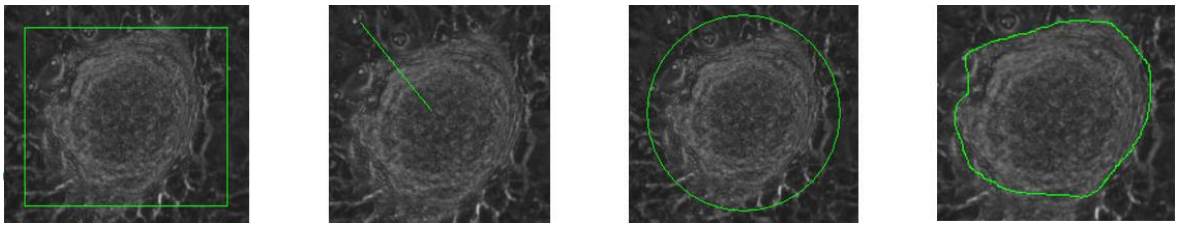

Figure 6. *Examples of the different ROIs geometries*

The possibility of tracking multiple ROIs simultaneously gave rise to the last tool developed for the software: mesh analysis. This tool allows the analysis of the whole image by automatically dividing it into multiple ROIs with the same dimension, and gives the opportunity of studying contraction propagation by mapping the onsets of each ROI. (Figure 7)

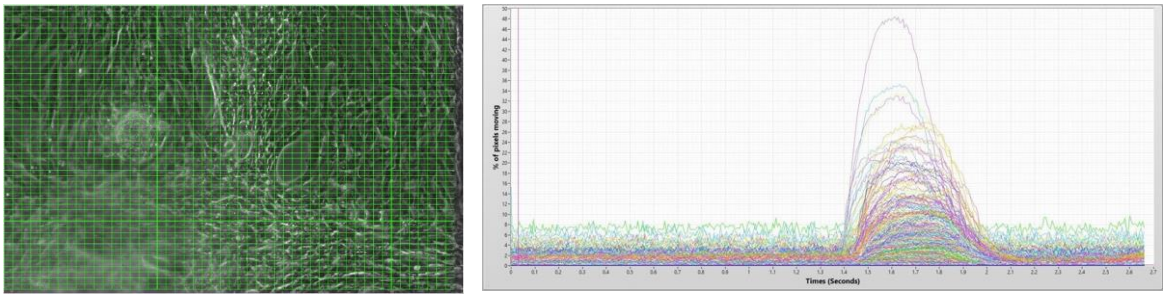

Figure 7. *Example of a 50x50 automatic mesh (left) and respective kinetic plot (right)*

Once the sample is analysed, the signal characteristics are analyzed using a conventional signal analysis program in Matlab programming language, that calculates the 10,50,90% of upstroke (rise) and a downstroke (fall) as well as 10-to-90 and 90-to-10 time and slew rate, and frequency, as described in the methods section.

3.2.2 Kinetic analysis of hPSC contraction during differentiation

Over time, there's a statistically significant decrease both in the spontaneous beating frequency (Figure 8A) and in the maximum percentage of moving pixels during contraction (Figure 8C). On the third week of culture, moreover, hPSC-CMs display the higher values of beat duration, followed by a decrease on days 28 and 35 (Figure 8B). As the differentiation continues, it was also observed a falling trend in the slew rate percentage during the contraction phase, although only on the fifth week there was a statistically significant decrease compared to the second week (Figure 8D). No trend was evident, instead, during the relaxation phase (Figure 8E).

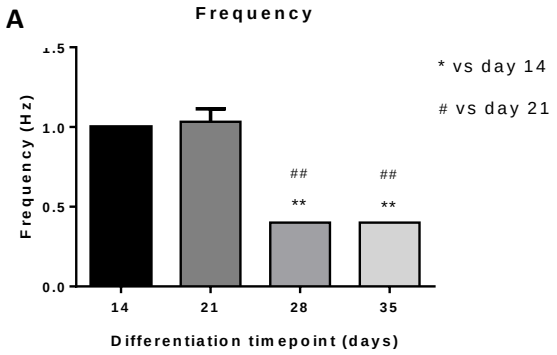

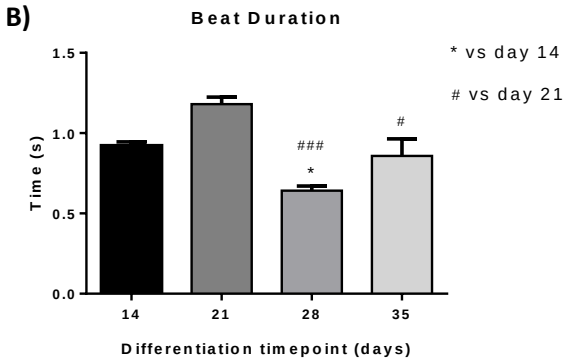

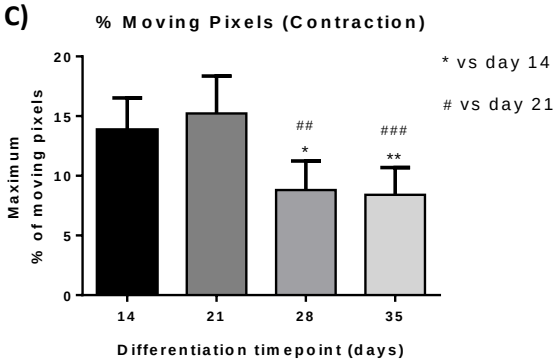

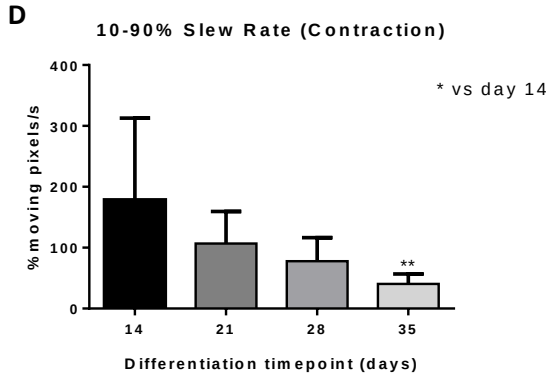

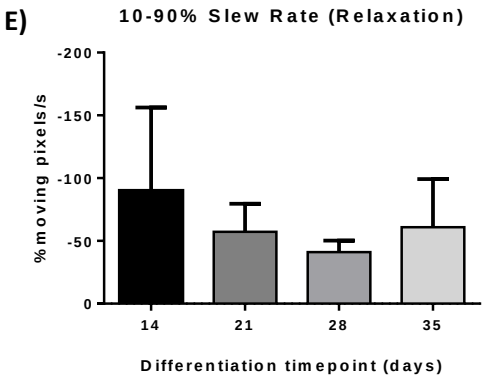

Figure 8. *Contraction characterization of hPSC-CMs spontaneous beat, at different stages of differentiation. A) Frequency. B) Beat Duration. C) Percentage of moving pixels at the peak of the contraction. D-E) Slew rate during contraction and relaxation.*
**p<0.05, **p<0.01, ##p<0.01, ###p<0.001*

3.2.3 Kinetic assessment following ß-adrenergic stimulation

To induce alterations in the contraction pattern and produce a chronotropic effect we treated hPSC-CMs with 1uM of Isoproterenol, and their beating activity was following recorded from 5' to 30' minutes after drug administration.

14th Day of differentiation

In the early stage of the differentiation, hPSC-CMs displayed an increase in the frequency of the spontaneous beating activity only after 15' of treatment with 1uM of Isoproterenol (Figure 9A), but only after 30' a decrease in the mean beat duration was noticeable (Figure 9B). On the other hand, the remaining parameters -maximum percentage of moving pixels during contraction and the slew rate percentage on both contraction and relaxation- displayed no significant trend (Figure 9C-E)

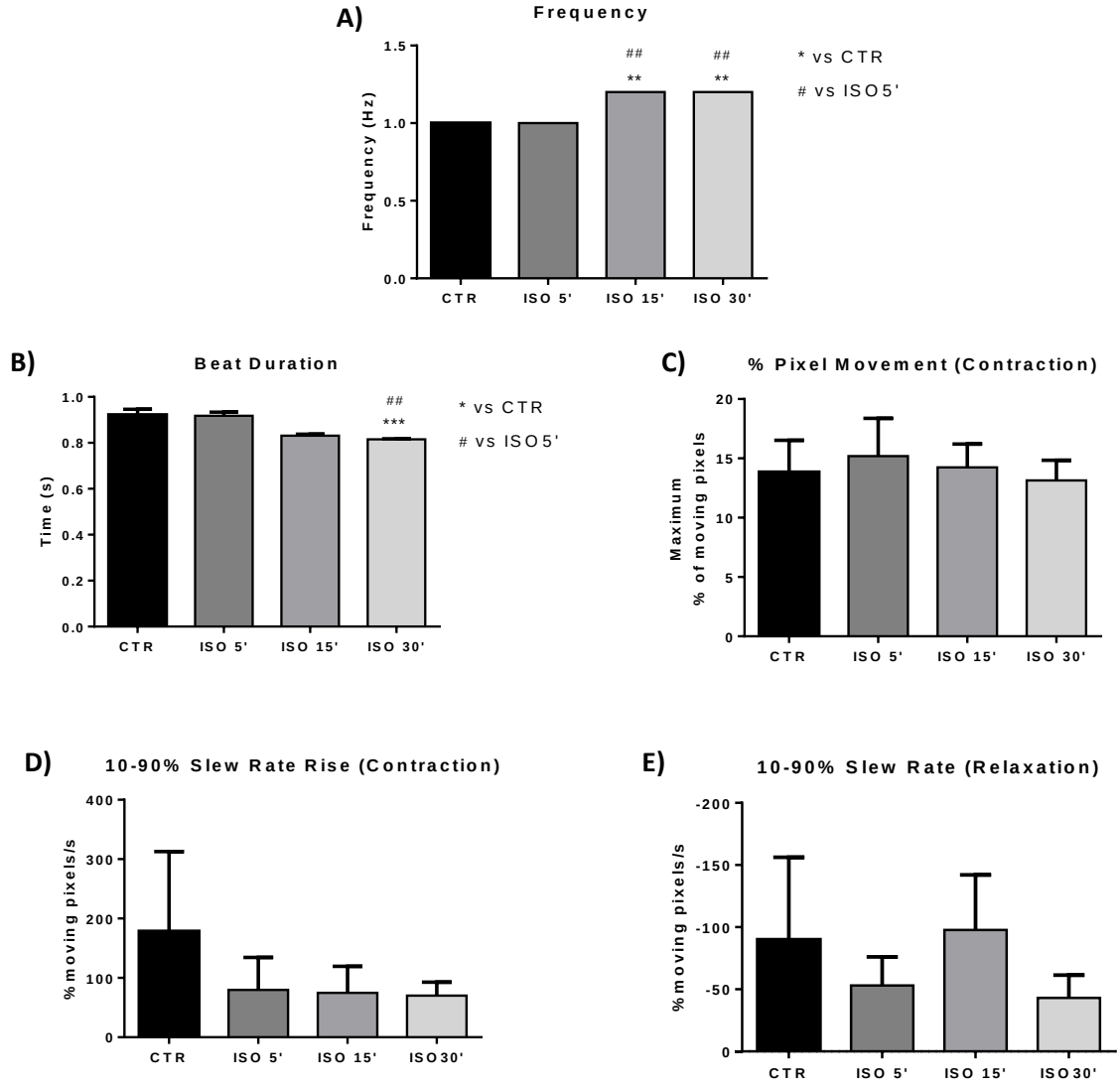

Figure 9. *Contraction characterization of hPSC-CMs at an early stage of differentiation (14th day), after treatment with 1uM of Isoproterenol. A) Frequency. B) Beat Duration. C) Percentage of moving pixels at the peak of the contraction. D-E) Slew rate during contraction and relaxation.*
***p<0.01, ##p<0.05, ***p<0.001*

21st Day of differentiation

After two weeks of culture hPSC-CMs responded to Isoproterenol (1uM) by increasing both the beating frequency and slew rate of contraction, and simultaneously decreasing the beat duration after 30' of treatment. On the contrary, no significant difference was recorded on the maximum percentage of moving pixels or in the relaxation slew rate (Figure 10).

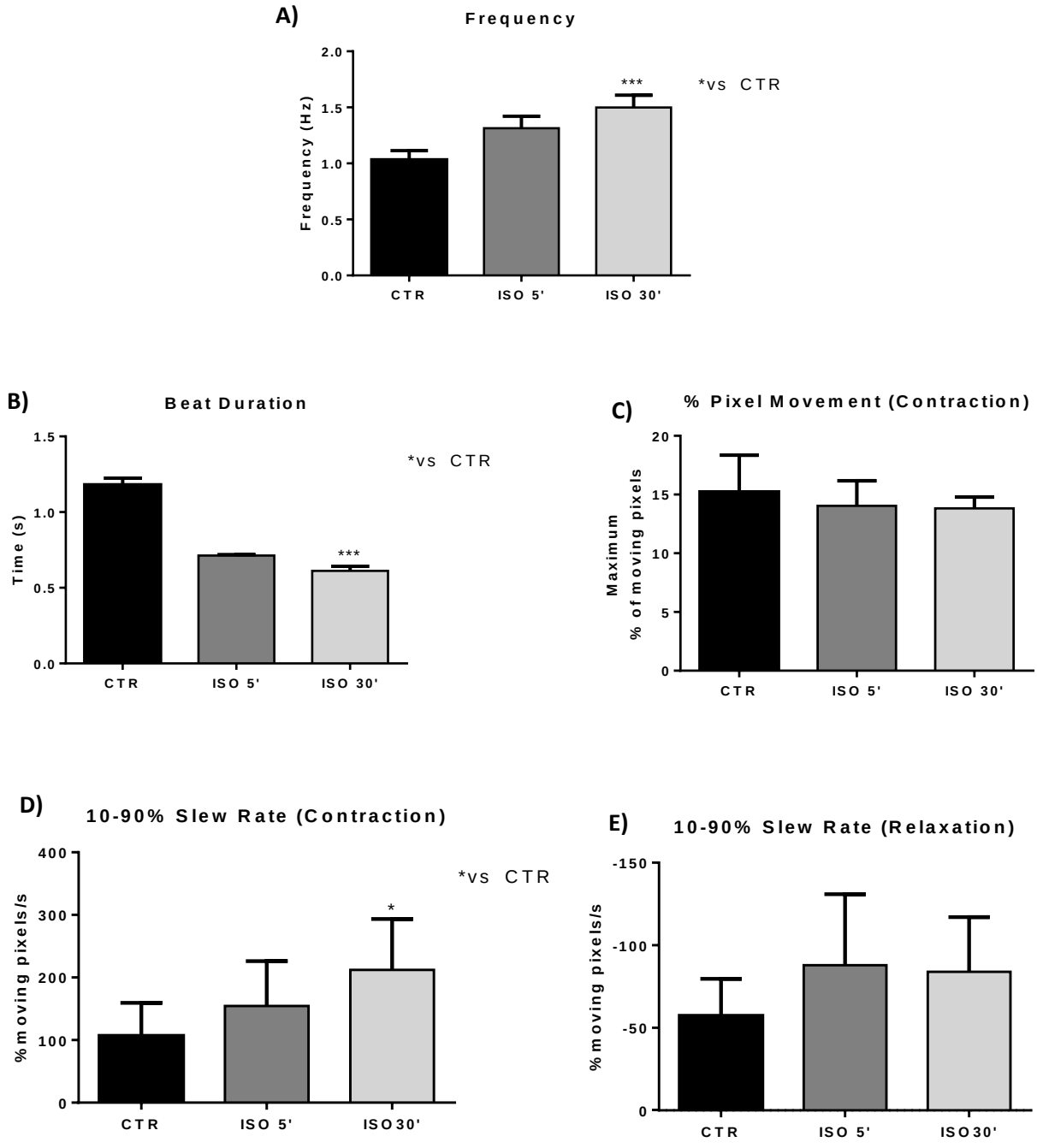

Figure 10. *Contraction characterization of hPSC-CMs on the third week of differentiation (D21), after treatment with 1uM of Isoproterenol. A) Frequency. B) Beat Duration. C) Percentage of moving pixels at the peak of the contraction. D-E) Slew rate during contraction and relaxation.*
**p<0.05, ***p<0.001*

28st Day of differentiation

On the fourth week of differentiation, hPSC-CMs, Isoproterenol treatment effectively increased cells beating frequency (Figure 11A) but left substantially unaltered the remaining parameters, besides beat duration that was significantly higher after 15' from the treatment (Figure 11B).

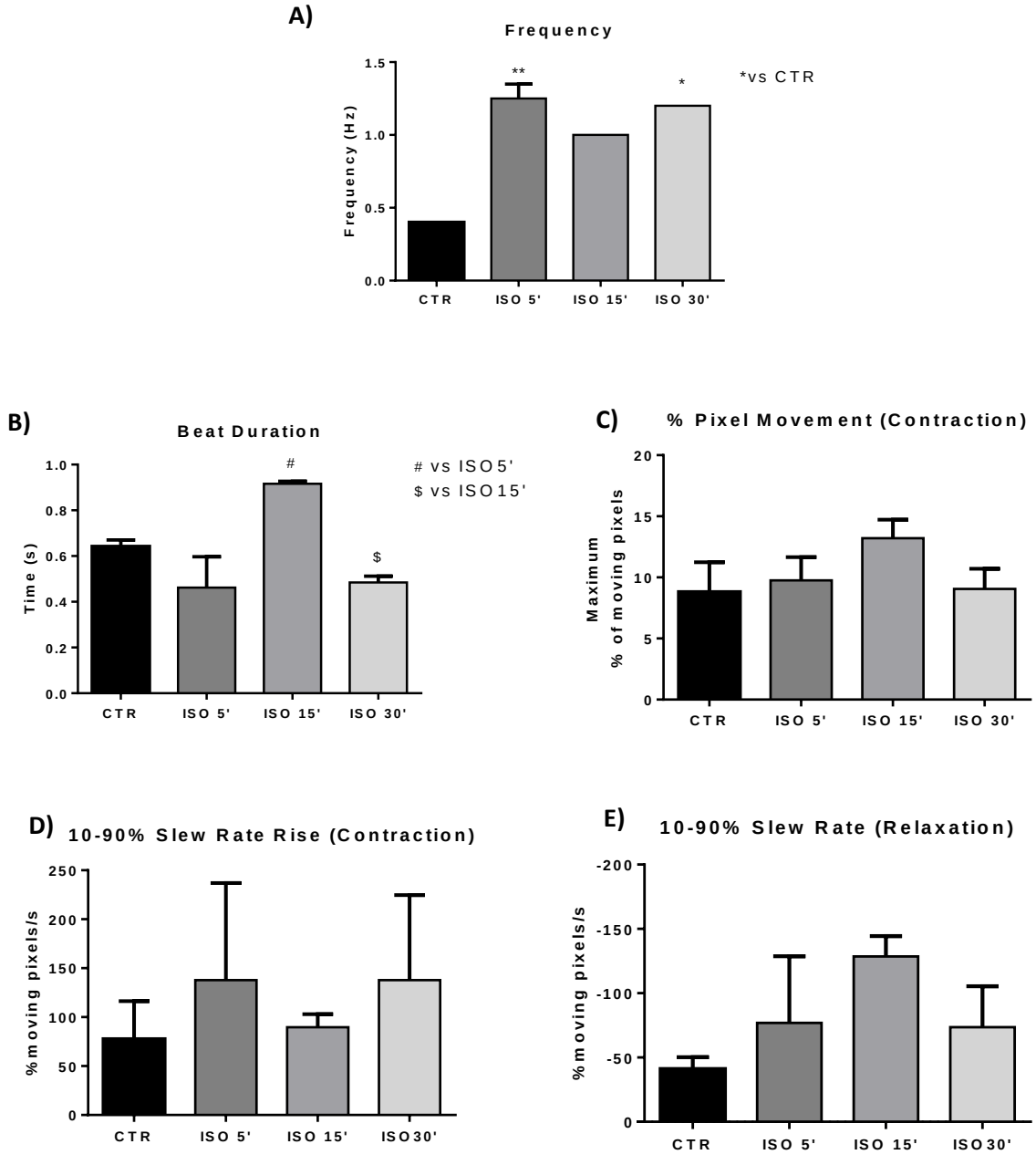

Figure 11. *Contraction parameters of 28 days-old hPSC-CMs, after treatment with 1uM of Isoproterenol. A) Frequency. B) Beat Duration. C) Percentage of moving pixels at the peak of the contraction. D-E) Slew rate during contraction and relaxation.*
**p<0.05, $^{\#}$p<0.05, $^{\$}$p<0.05, **p<0.05*

35th Day of differentiation

5 days-old hPSC-CMs once again proved to be sensitive to the isoproterenol chronotropic effect, as can be observed in Figure 12A. At this stage of differentiation, the frequency increase is accompanied by a decrease in the beat duration, at all the time points, and an increase in the contraction slew rate after 30' of treatment.

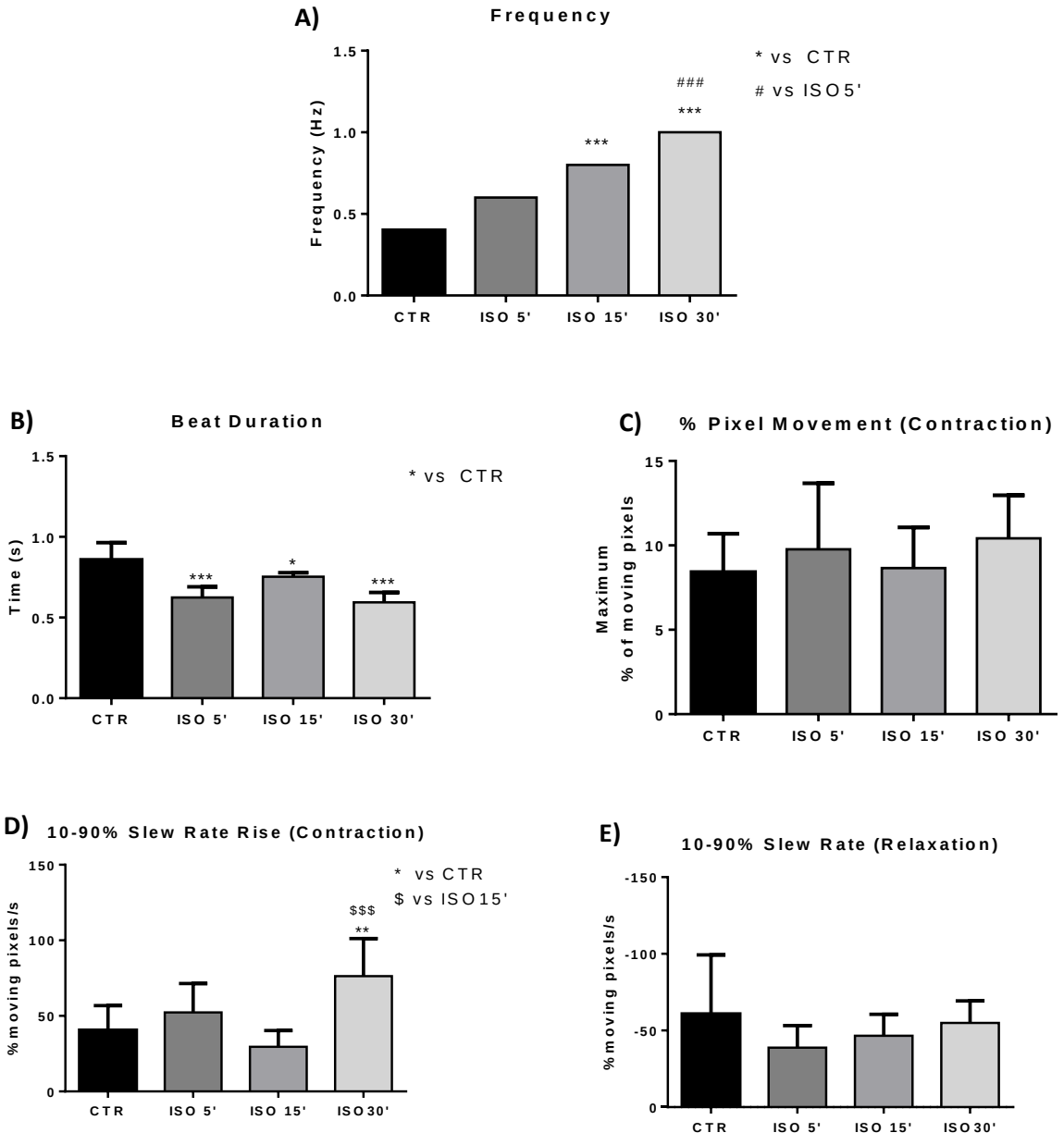

Figure 12. *Contraction parameters of 35 days-old hPSC-CMs, after treatment with 1uM of Isoproterenol. A) Frequency. B) Beat Duration. C) Percentage of moving pixels at the peak of the contraction. D-E) Slew rate during contraction and relaxation. *p<0.05, **p<0.01, ***p<0.001, $^{\$\$\$}$p<0.001*

3.2.4 Paradoxical mechanical hyper-coupling in differentiated beating bodies

Qualitative observation of differentiating hPSC-CMs draws attention to the presence of differentiated beating clusters that are physically connected by non-beating cells. However, some clusters in the same field of view are mechanically synchronous albeit the distance between each other suggests that non-beating cells are certainly active in supporting propagation (Figure 13).

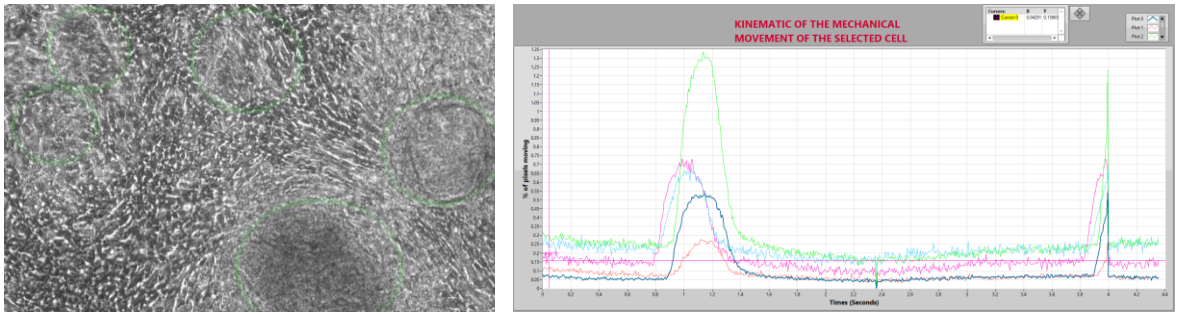

Figure 13. *Mechanical synchronicity in five beating bodies from the same Field of View. Selected ROIs on the left panel and relative plot of contraction/relaxation (right).*

Therefore, the mechanical synchronicity in ca. 30 coupled clusters was analyzed by comparing the signals from the "trigger" clusters (Source) and the "receipt" clusters (Sink).

The considered parameters were upstroke velocity, the time at 10-50-90% of signal rise (contraction) as well as the area under the curve (AUC) as an indirect index of total energy expenditure and the beat duration for both source and sink clusters (n=30 couples). Interestingly while we did not observe any modification for the upstroke velocity and AUC, we observed a significant reduction for the time necessary to reach 10, 50 and 90% of the peak (Figure 14).

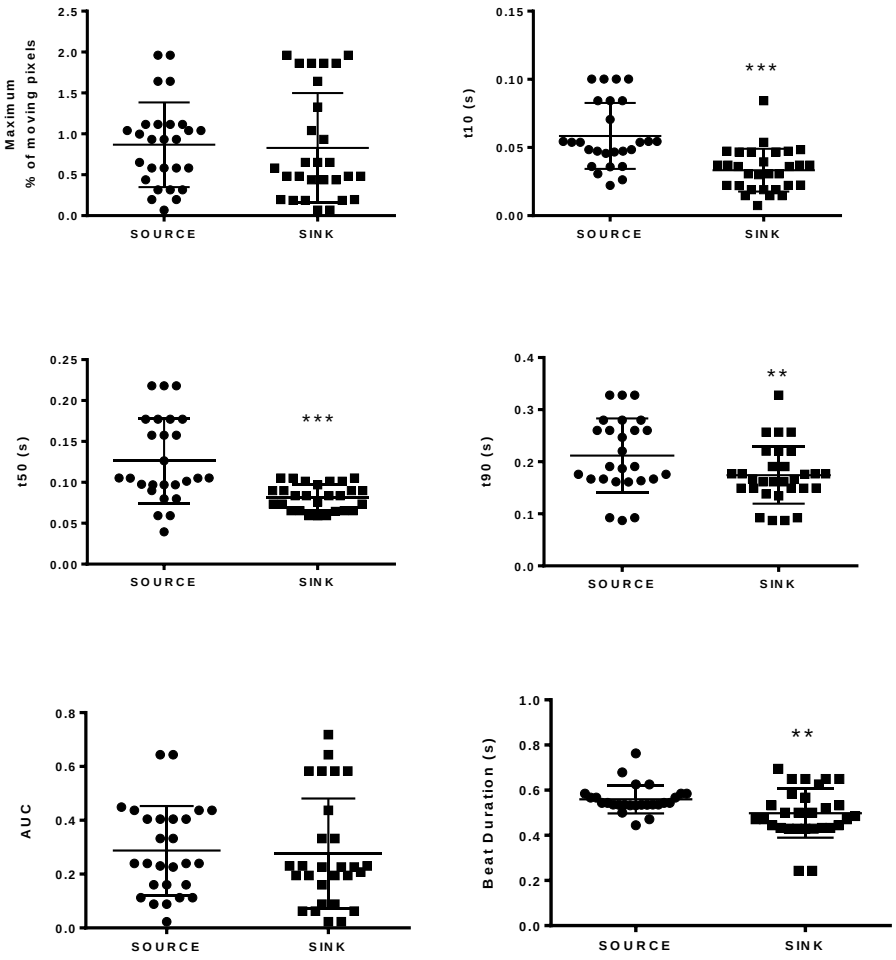

Figure 20. *Kinetic analysis of source and sink beating clusters. **p<0.01, ***p<0.001*

Another finding concerned spatiotemporal sink-source dependency (Figure 21). Plotting the distance between clusters and the difference between the relative t10 points, no linear dependency was found (R=0.05).

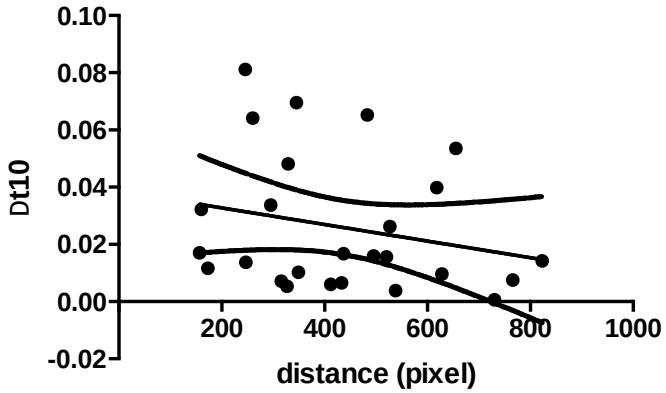

Figure 21. *Sink-source spatiotemporal dependency calculated as $t10_{sink} - t10_{source}$ plotted vs distance.*

4. DISCUSSION

One of the main factors affecting the efficiency of hPSCs differentiation into cardiomyocytes is the relative cell confluence at the onset of the differentiation protocol. Following a brief set up of the optimal confluence range, cardiomyocytes were successfully differentiated following the manufacturer's indications (Cardiomyocyte differentiation kit, Thermo Fisher). The obtained cell population presented spontaneous beating activity around days 7-12 and tested positive for cardiomyocytes' markers α-actinin and Troponin I in immunofluorescence assays.

During the initial stages of differentiation, hPSC-CMs organize in beating monolayers that are poorly characterized in terms of their kinetics. The conventional and available software does not allow the possibility to continuously mechanically monitor a specific sample for a given time; moreover, those software are not user-friendly and are skill-operator dependent. For example, Musclemotion [89], a plugin for ImageJ, does not allow the acquisition of more than one ROI thus limiting the study of impulse propagation across a wide area of a beating monolayer, as suggested by the mesh analysis tool (Figure 7). Similar Ionoptix technique [90] requires a proper sarcomere organization or edge-detection for measuring contractility and cannot be suitable for beating monolayers.

Our developed processing software (LOKI) is completely operator-independent as the crucial steps (Threshold adjustment, Image segmentation, mesh production, etc.) are fully automatic. LOKI does not require edge detection and can be applicable for a plethora of beating cells, from hiPSC-CM, neonatal, adult cardiomyocytes and potentially to the *in-vivo* beating heart.

Through non-invasive video-based analysis of the cell culture, this work aimed to shed some light on the contractile behaviour of these monolayers at different stages of differentiation and in response to external stimuli, such as drug treatments.

For differentiation analysis, hPSC-CMs beating monolayers were evaluated weekly. In basal conditions, with no treatment or electrical stimulation, it was observed a decline in the main parameters characterizes the contraction pattern, over time. There's a fall in the frequency of the spontaneous beats, and a decrease both in the percentage of moving pixels (proportional to the monolayers' movement) and in the slope of the upstroke phase; furthermore, after the 21st day, a shortening of beat duration is observed. Qualitative observation of the contraction profiles revealed that at early stages of differentiation (D14 and D21) cells display a plateau after the maximum contraction. This can also be evinced from the abovementioned parameters since D14 and D21 profiles are characterized by longer beat durations despite their high values of contraction slew rates and their average relaxation slope.

Data on Isoproterenol treatment collected at different time points of the differentiation revealed that the hPSC-CMs line employed is effectively sensitive to the chronotropic effect of adrenergic stimulation, as demonstrated by the rise in the beating frequency after treatment, although the impact is more pronounced at later stages of differentiation when the spontaneous beating activity previous treatment displays lower frequency values. Furthermore, at the 4 differentiation time points studied the parameters that characterize the cardiomyocyte contraction vary differently in response to the increased frequency. On the second week of differentiation, when the basal frequency is already high and long beating durations are recorded, the further frequency increase necessarily requires a decrease of beating duration. The same occurs on the 21st and 35th day of differentiation with an additional increase of the upstroke velocity (the contraction slew rate). To note, on the 4th week of differentiation, instead, no clear trend of the parameters is recorded: beat duration even increases after 15' of treatment, but no increase in contraction slew rate is recorded, nor a decrease in the maximum percentage of pixel movement, suggesting that the rise in the beating frequency is merely obtained by shortening the time between peaks. Those data are important in understanding the answer from hPSC-CMs on ß-adrenergic stimulation during differentiation. Mechanical signals can be indeed a novel functional index of differentiation quality for hPSC-CMs, especially in the context of inherited contractile cardiomyopathies such as (RyR2 mutations, hypoplasic left ventricular syndrome, etc.). Further data on hPSC-CMs that recapitulate that phenotypes are ongoing in the lab.

Lastly, the role and the presence of mechanical propagation in hPSC-CM monolayer need to be assessed; in particular, it would be interesting to study the interaction between electrical propagation and mechanical waves in experimental conditions where either electrical or mechanical coupling are pharmacologically blocked. The presence of mechanical waves that support electrical propagation in the heart (soliton theory) fascinated the scientists that wanted to revisit the Hodgkin-Huxley theory. Indeed, biological membranes due to their elastic properties and their relationship with temperature are capable to propagate localized mechanical perturbation. [91] This has been described by mathematical models,[92] in neurons[93] and in-vivo heart by fast ultrasound imaging.[94]

Qualitative observations on the mechanical synchronization of distanced clusters surrounded by non-beating cells suggest that this cell population is certainly active in supporting propagation. This contrasts with the electrotonic impulse propagation theory (supported by thousands of in-vitro experiments), whereby electrotonic action potential propagation cannot be supported for a distance over the cardiac space constant in passive cells or nano bridges(e.g 350-360 μm) [95,96]

Further preliminary data suggest that the mechanical propagation between clusters cannot be driven only by a passive electrotonic wave: indeed, it was observed a significant reduction for the time necessary to reach 10, 50 and 90% of the contraction part of the curve. Furthermore, no linear dependence was observed between the distance between clusters and contraction onset (considered

the t10), suggesting that not only electrical propagation may play a role in supporting synchronization, but mechanical waves may sustain electrical propagation at this stage of differentiation, as well.

Therefore, future investigation focused on decoupling electrical and mechanical waves, could elucidate whether soliton plays a role in hPSC-CMs during and after differentiation and if its modulation may benefit differentiated hPSC-CMs at later stages.

CONCLUSION

The proposed software for contraction recording efficiently detected hPSC-CMs beating activity and its variations related to cell maturation and pharmacological treatment with a β-adrenergic agonist. The analysis algorithm provided a detailed characterization of the contraction signal, with several parameters that are likely affected in different pathophysiological conditions. Furthermore, the possibility of selecting multiple ROIs, proved valuable when studying synchronization across a large field; in particular, the novel feature of mesh analysis, not yet applied, holds great potential in the study of contractile waves propagation through monocellular or heterocellular monolayers.

Nevertheless, working on the development of software for cardiomyocytes contraction evaluation and unveiling the underlying mechanisms of imaging analysis has brought to light the current limits of pure video-based approaches.

Despite several works proving the correlation between kinetic and kinematic parameters, provided by different technologies, with gold standard functional analysis, a breakthrough in the understanding of the output is missing. Current strategies successfully reflect cardiomyocytes' movement in terms of amplitude, direction and timing, however, limiting the contraction phenomenon to these characteristics and possibly defining its velocity, fails to finalize their translation to further physical parameters such as cardiomyocytes' force and energy. Furthermore, the most versatile tracking strategies, that ensure a feasible translation among models, return parameters in arbitrary units. This not only prevents the comparison between different models but also limits the understanding of these parameters' scalability in progressively organized structures (from a single cell to tissue and finally organ). As a result, the information deriving from a flat monolayer is not comparable to the information obtained from a multilayer cluster, thus arising the need for a de-normalization of data; to do so, a systematic and accurate characterization of different morphologies needs to be performed, accurately considering characteristics, such as cell density, role in the contraction (defining whether field analysed a source of contraction, or is merely stretched) and adhesion (identifying whether the movement is constrained or not).

This being said, the video-based analysis still holds great potential for *in vitro* drug testing; the simplicity and automatization possibilities make this analysis easily scalable to high-throughput assays, and the technology underneath is sensitive enough to detect variations affecting the frequency, amplitude and contraction velocity, as long as proper control conditions are included. The challenge for this field now consists in deepening the information behind the pure pixel, integrating it with complementary data concerning the substrate identity and composition.

APPENDIX 1

Guide User Interface of LOKI Software analysis

FILE AND PROPERTIES SELECTION

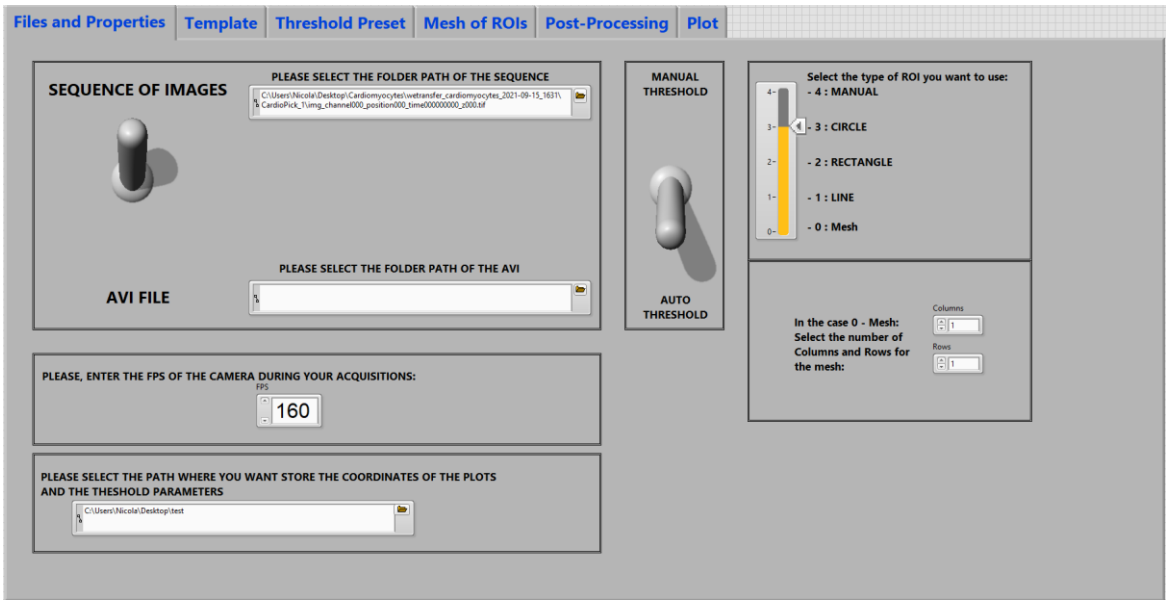

Figure 1S. *The first panel (File and Properties) represents the selection of images folder, the metadata folder and the geometry of the ROI's selection.*

TEMPLATE IMAGE REFERENCE SELECTION

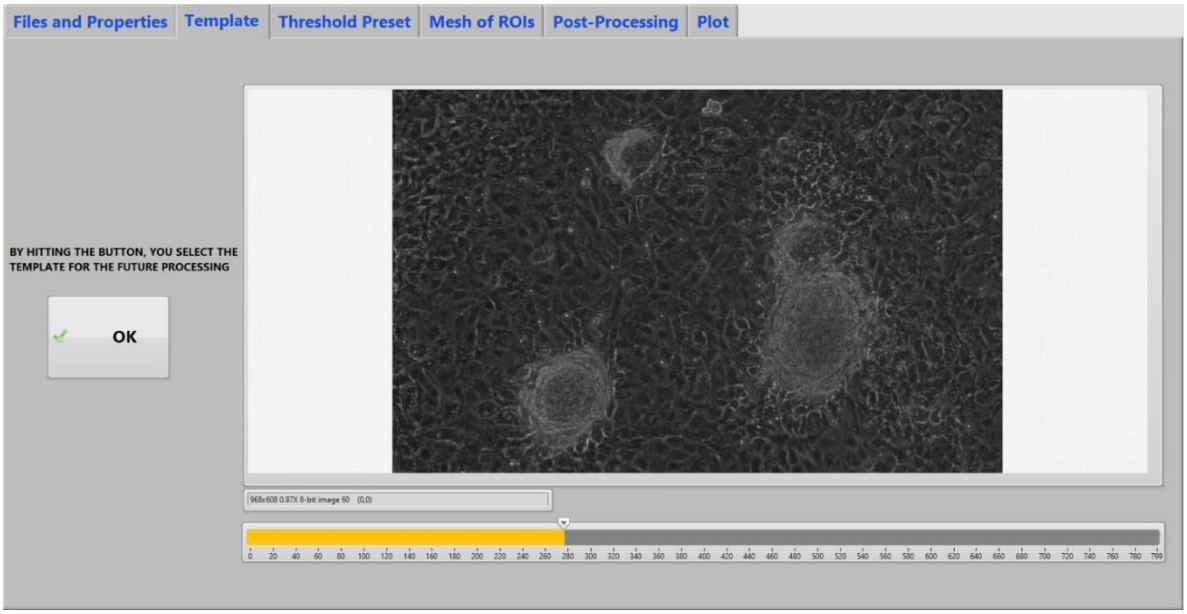

Figure 2S. *The second panel (Template) allows the selection of the reference frame*

THRESHOLD SELECTION

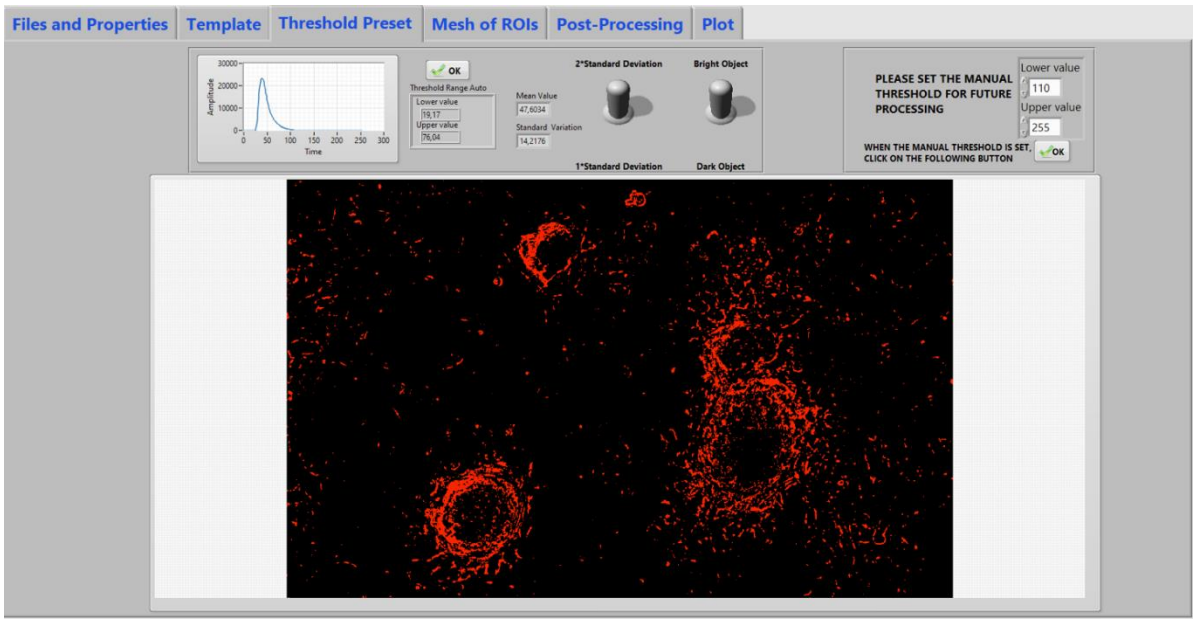

Figure 3S. *The third panel (Threshold Preset) represents the selection of automated or manual Threshold. The automated threshold depends on the distributed value of the central limit theory for standard deviation of the mean.*

ROIs SELECTION

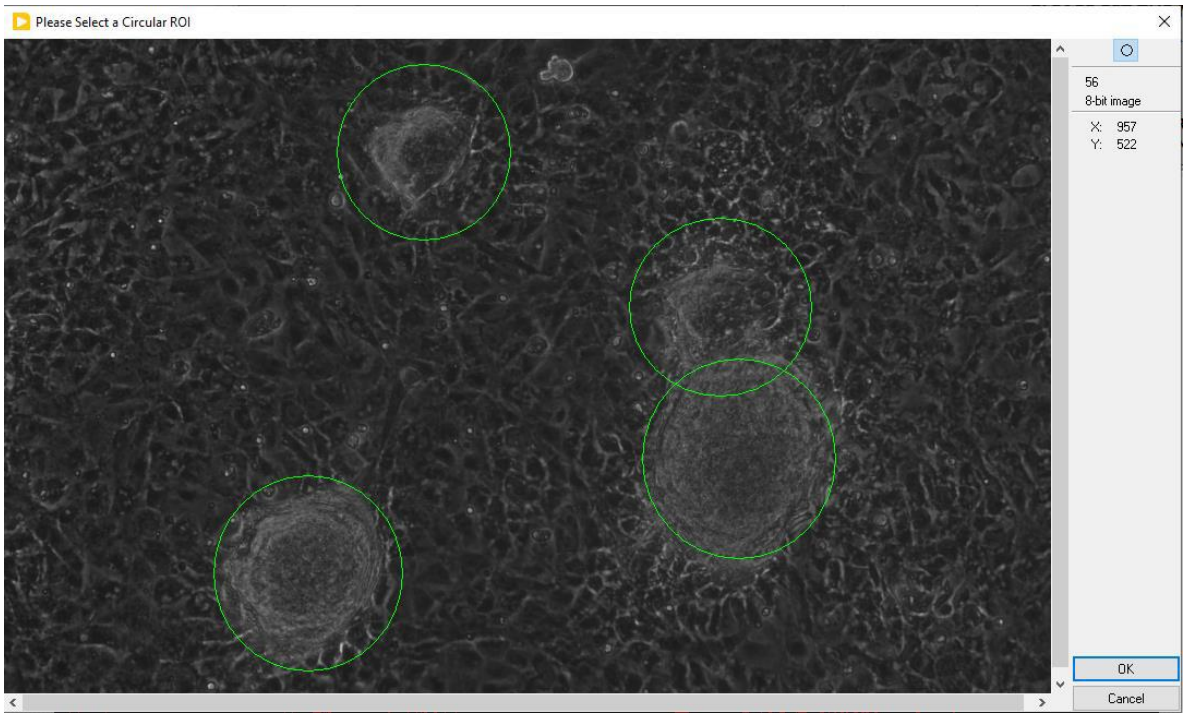

Figure 4S. *The fourth panel represents the selection of ROI's.*

PROCESSING

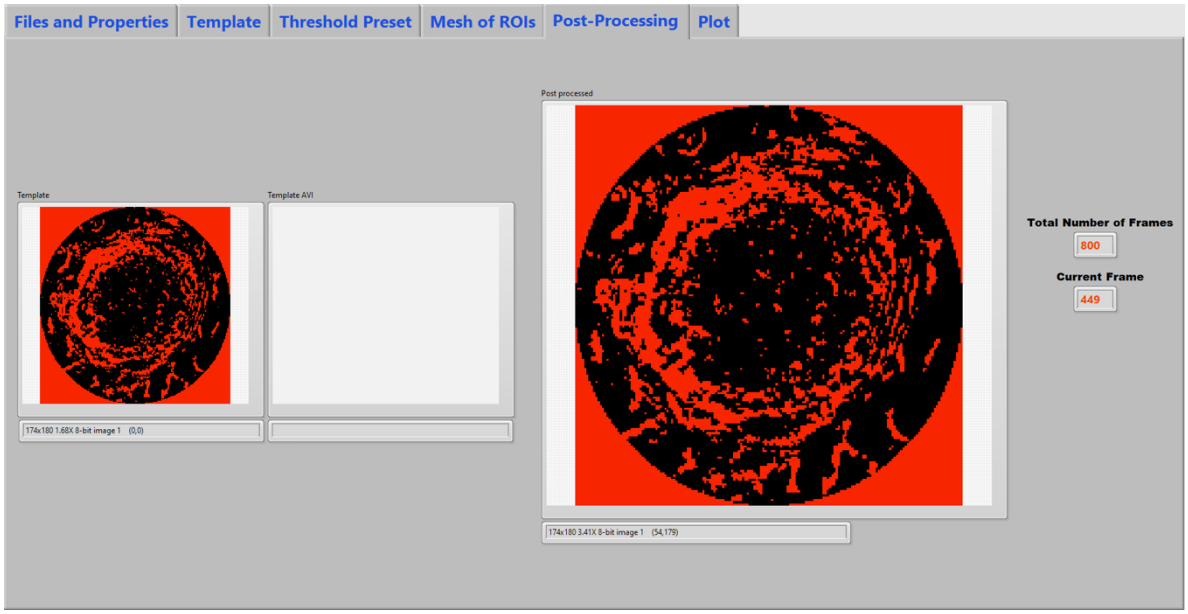

Figure 5S. *The fifth panel represents the processing of each selected ROI's (here is represented the ROI1 – lower left from the previous image)*

PLOT REPRESENTATION

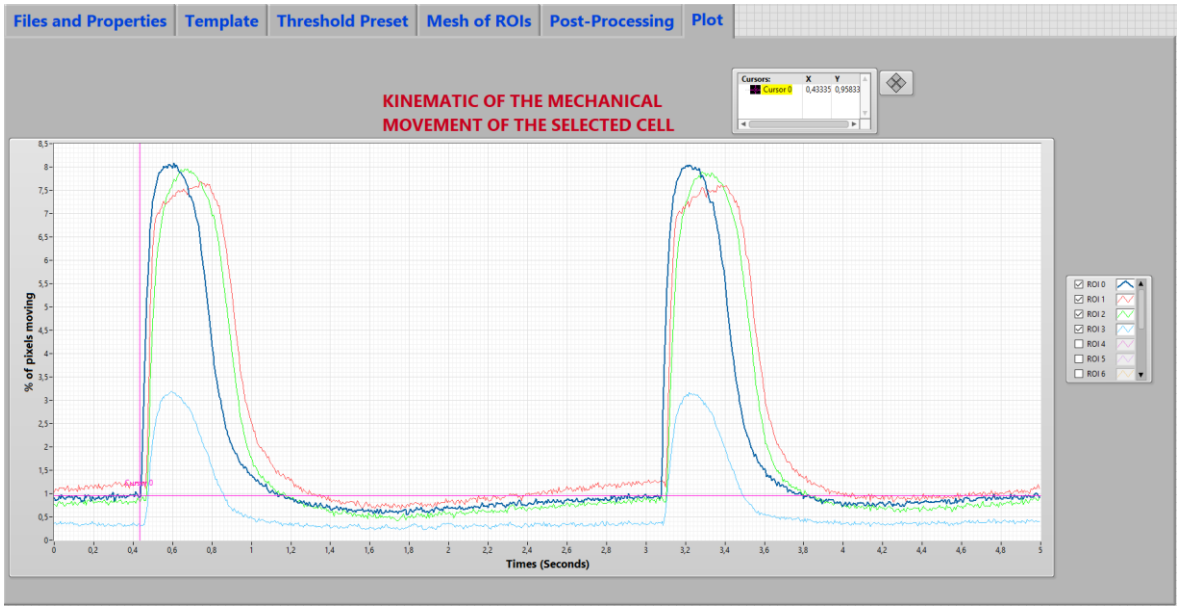

Figure 13. *The sixth panel represents the mechanical plot of each selected ROI's. Upstroke: contraction; downstroke: relaxation*

Afterward, the signal characteristics were analyzed using a conventional signal analysis program in Matlab Environment, calculating the 10,50,90% of upstroke (rise) and a downstroke (fall) as well as 10-to-90 and 90-to-10 time, frequency, and AUC as described in the method section.

BIBLIOGRAPHY

1. Mensah, G. A., Roth, G. A. & Fuster, V. The Global Burden of Cardiovascular Diseases and Risk Factors: 2020 and Beyond. *Journal of the American College of Cardiology* **74**, 2529–2532 (2019).

2. Cardiovascular diseases (CVDs). https://www.who.int/news-room/fact-sheets/detail/cardiovascular-diseases-(cvds).

3. Page, R. L. *et al.* Drugs That May Cause or Exacerbate Heart Failure: A Scientific Statement From the American Heart Association. *Circulation* **134**, e32–e69 (2016).

4. Christine Mummery, C. L., Sala, L., Bellin, M. & Mummery, C. L. Themed Section: New Insights into Cardiotoxicity Caused by Chemotherapeutic Agents Integrating cardiomyocytes from human pluripotent stem cells in safety pharmacology: has the time come? (2016) doi:10.1111/bph.v174.21/issuetoc.

5. Ewer, M. S. & Ewer, S. M. Cardiotoxicity of anticancer treatments. *Nature Reviews Cardiology 2015 12:9* **12**, 547–558 (2015).

6. Cross, M. J. *et al.* Physiological, pharmacological and toxicological considerations of drug-induced structural cardiac injury. *British Journal of Pharmacology* **172**, 957 (2015).

7. Varga, Z. v., Ferdinandy, P., Liaudet, L. & Pacher, P. Drug-induced mitochondrial dysfunction and cardiotoxicity. *American journal of physiology. Heart and circulatory physiology* **309**, H1453–H1467 (2015).

8. Paloschi, V. *et al.* Organ-on-a-chip technology: a novel approach to investigate cardiovascular diseases. *Cardiovascular Research* **117**, 2742–2754 (2021).

9. 2011 ACCF/AHA guideline for the diagnosis and treatment of hypertrophic cardiomyopathy: A report of the American College of Cardiology Foundation/American Heart Association Task Force on Practice Guidelines Developed in Collaboration with the American Association for Thoracic Surgery, American Society of Echocardiography, American Society of Nuclear Cardiology, Heart Failure Society of America. *Journal of the American College of Cardiology* **58**, (2011).

10. Kathiresan, S. & Srivastava, D. Genetics of Human Cardiovascular Disease. *Cell* **148**, 1242–1257 (2012).

11. Tanai, E. & Frantz, S. Pathophysiology of Heart Failure Definition and Epidemiology. *Compr Physiol* **6**, 187–214 (2016).

12. Greenberg, M. J. & Tardiff, J. C. Complexity in genetic cardiomyopathies and new approaches for mechanism-based precision medicine. (2021) doi:10.1085/jgp.202012662.

13. Baldwin, W. M., Su, C. A., Shroka, T. M. & Fairchild, R. L. Experimental Models of Cardiac Transplantation - design determines relevance. *Current opinion in organ transplantation* **19**, 525 (2014).

14. Knight, W. E. *et al.* Ex vivo Methods for Measuring Cardiac Muscle Mechanical Properties. *Frontiers in Physiology* **11**, 1756 (2021).

15. Louch, W. E., Sheehan, K. A. & Wolska, B. M. Methods in cardiomyocyte isolation, culture, and gene transfer. *Journal of Molecular and Cellular Cardiology* vol. 51 288–298 (2011).

16. Parameswaran, S., Kumar, S., Verma, R. S. & Sharma, R. K. Cardiomyocyte culture - an update on the in vitro cardiovascular model and future challenges. *Canadian journal of physiology and pharmacology* vol. 91 985–998 (2013).

17. Honjo, H., Boyett, M. R., Kodama, I. & Toyama, J. Correlation between electrical activity and the size of rabbit sino-atrial node cells. *The Journal of physiology* **496 (Pt 3)**, 795–808 (1996).

18. Xu, X. & Colecraft, H. M. Primary culture of adult rat heart myocytes. *Journal of visualized experiments : JoVE* (2009) doi:10.3791/1308.

19. Mitcheson, J. S., Hancox, J. C. & Levi, A. J. Cultured adult cardiac myocytes: future applications, culture methods, morphological and electrophysiological properties. *Cardiovascular research* **39**, 280–300 (1998).

20. Powell, T. & Twist, V. W. A rapid technique for the isolation and purification of adult cardiac muscle cells having respiratory control and a tolerance to calcium. *Biochemical and Biophysical Research Communications* **72**, 327–333 (1976).

21. Li, H. *et al.* Optimized Langendorff perfusion system for cardiomyocyte isolation in adult mouse heart. *Journal of Cellular and Molecular Medicine* **24**, 14619 (2020).

22. Ackers-Johnson, M. *et al.* A Simplified, Langendorff-Free Method for Concomitant Isolation of Viable Cardiac Myocytes and Nonmyocytes from the Adult Mouse Heart. *Circulation Research* **119**, 909–920 (2016).

23. Graham, E. L. *et al.* Isolation, culture, and functional characterization of adult mouse cardiomyoctyes. *Journal of visualized experiments : JoVE* (2013) doi:10.3791/50289.

24. Zhou, Y. Y. *et al.* Culture and adenoviral infection of adult mouse cardiac myocytes: Methods for cellular genetic physiology. *American Journal of Physiology - Heart and Circulatory Physiology* **279**, 429–436 (2000).

25. The effects of divalent cations on the ultrastructure of the perfused rat heart. *Journal of anatomy* **101**, 239–261 (1967).

26. Mitcheson, J. S., Hancox, J. C. & Levi, A. J. Cultured adult cardiac myocytes: Future applications, culture methods, morphological and electrophysiological properties. *Cardiovascular Research* **39**, 280–300 (1998).

27. Boateng, S. Y. *et al.* RGD and YIGSR synthetic peptides facilitate cellular adhesion identical to that of laminin and fibronectin but alter the physiology of neonatal cardiac myocytes. *American Journal of Physiology - Cell Physiology* **288**, 30–38 (2005).

28. Vanwinkle, W. B., Snuggs, M. B. & Buja, L. M. Cardiogel: a biosynthetic extracellular matrix for cardiomyocyte culture. *In vitro cellular & developmental biology. Animal* **32**, 478–485 (1996).

29. Piper, H. M., Jacobson, S. L. & Schwartz, P. Determinants of cardiomyocyte development in long-term primary culture. *Journal of molecular and cellular cardiology* **20**, 825–835 (1988).

30. Louch, W. E. *et al.* Reduced synchrony of Ca2+ release with loss of T-tubules - A comparison to Ca2+ release in human failing cardiomyocytes. *Cardiovascular Research* **62**, 63–73 (2004).

31. Leach, R. N., Desai, J. C. & Orchard, C. H. Effect of cytoskeleton disruptors on L-type Ca channel distribution in rat ventricular myocytes. *Cell Calcium* **38**, 515–526 (2005).

32. Banyasz, T. *et al.* Transformation of adult rat cardiac myocytes in primary culture. *Experimental Physiology* **93**, 370–382 (2008).

33. Akuzawa-Tateyama, M., Tateyama, M. & Ochi, R. Sustained beta-adrenergic stimulation increased L-type Ca2+ channel expression in cultured quiescent ventricular myocytes. *The journal of physiological sciences : JPS* **56**, 165–172 (2006).

34. Holt, E., Lunde, P. K., Sejersted, O. M. & Christensen, G. Electrical stimulation of adult rat cardiomyocytes in culture improves contractile properties and is associated with altered calcium handling. *Basic research in cardiology* **92**, 289–298 (1997).

35. Ravi, V., Jain, A., Taneja, A., Chatterjee, K. & Sundaresan, N. R. Isolation and Culture of Neonatal Murine Primary Cardiomyocytes. *Current Protocols* **1**, e196 (2021).

36. Chlopcíková, S., Psotová, J. & Miketová, P. Neonatal rat cardiomyocytes--a model for the study of morphological, biochemical and electrophysiological characteristics of the heart. *Biomedical papers of the Medical Faculty of the University Palacky, Olomouc, Czechoslovakia* **145**, 49–55 (2001).

37. Fu, Z. *et al.* Enhanced toxicity and ROS generation by doxorubicin in primary cultures of cardiomyocytes from neonatal metallothionein-I/II null mice. *Toxicology in vitro : an international journal published in association with BIBRA* **24**, 1584–1591 (2010).

38. Qu, Z. *et al.* Attenuation of the upregulation of NF-κB and AP-1 DNA-binding activities induced by tunicamycin or hypoxia/reoxygenation in neonatal rat cardiomyocytes by SERCA2a overexpression. *International journal of molecular medicine* **47**, (2021).

39. Yamashita, N. *et al.* Induction of manganese superoxide dismutase in rat cardiac myocytes increases tolerance to hypoxia 24 hours after preconditioning. *The Journal of clinical investigation* **94**, 2193–2199 (1994).

40. Date, T. *et al.* Adenovirus-mediated expression of p35 prevents hypoxia/reoxygenation injury by reducing reactive oxygen species and caspase activity. *Cardiovascular research* **55**, 309–319 (2002).

41. Claycomb, W. C. & Palazzo, M. C. Culture of the terminally differentiated adult cardiac muscle cell: A light and scanning electron microscope study. *Developmental Biology* **80**, 466–482 (1980).

42. Davidson, M. M. *et al.* Novel cell lines derived from adult human ventricular cardiomyocytes. *Journal of Molecular and Cellular Cardiology* **39**, 133–147 (2005).

43. Claycomb, W. C. *et al.* HL-1 cells: a cardiac muscle cell line that contracts and retains phenotypic characteristics of the adult cardiomyocyte. *Proceedings of the National Academy of Sciences of the United States of America* **95**, 2979–2984 (1998).

44. Steinhelper, M. E. *et al.* Proliferation in vivo and in culture of differentiated adult atrial cardiomyocytes from transgenic mice. *The American journal of physiology* **259**, (1990).

45. White, S. M., Constantin, P. E. & Claycomb, W. C. Cardiac physiology at the cellular level: use of cultured HL-1 cardiomyocytes for studies of cardiac muscle cell structure and function. *American journal of physiology. Heart and circulatory physiology* **286**, (2004).

46. Zhang, X. *et al.* MicroRNA-195 Regulates Metabolism in Failing Myocardium Via Alterations in Sirtuin 3 Expression and Mitochondrial Protein Acetylation. *Circulation* **137**, 2052–2067 (2018).

47. Zhang, J. *et al.* SYVN1/GPX5 axis affects ischemia/reperfusion induced apoptosis of AC16 cells by regulating ROS generation. *American journal of translational research* **13**, 4055–4067 (2021).

48. Caspi, O. *et al.* Tissue engineering of vascularized cardiac muscle from human embryonic stem cells. *Circulation Research* **100**, 263–272 (2007).

49. Kadota, S. *et al.* Development of a reentrant arrhythmia model in human pluripotent stem cell-derived cardiac cell sheets. *European Heart Journal* **34**, 1147–1156 (2013).

50. Mummery, C. L. *et al.* Differentiation of human embryonic stem cells and induced pluripotent stem cells to cardiomyocytes: A methods overview. *Circulation Research* **111**, 344–358 (2012).

51. van den Berg, C. W., Elliott, D. A., Braam, S. R., Mummery, C. L. & Davis, R. P. Differentiation of Human Pluripotent Stem Cells to Cardiomyocytes Under Defined Conditions. *Methods in Molecular Biology* **1353**, 163–180 (2014).

52. Lian, X. *et al.* Directed cardiomyocyte differentiation from human pluripotent stem cells by modulating Wnt/β-catenin signaling under fully defined conditions. *Nature protocols* **8**, 162–175 (2013).

53. Burridge, P. W. *et al.* Chemically defined generation of human cardiomyocytes. *Nature methods* **11**, 855–860 (2014).

54. Snir, M. *et al.* Assessment of the ultrastructural and proliferative properties of human embryonic stem cell-derived cardiomyocytes. *American journal of physiology. Heart and circulatory physiology* **285**, (2003).

55. Ma, J. *et al.* High purity human-induced pluripotent stem cell-derived cardiomyocytes: electrophysiological properties of action potentials and ionic currents. *American Journal of Physiology - Heart and Circulatory Physiology* **301**, H2006 (2011).

56. Veerman, C. C. *et al.* Immaturity of Human Stem-Cell-Derived Cardiomyocytes in Culture: Fatal Flaw or Soluble Problem? *Stem Cells and Development* **24**, 1035–1052 (2015).

57. Dolnikov, K. *et al.* Functional properties of human embryonic stem cell-derived cardiomyocytes: intracellular Ca2+ handling and the role of sarcoplasmic reticulum in the contraction. *Stem cells (Dayton, Ohio)* **24**, 236–245 (2006).

58. Ribeiro, M. C. *et al.* Functional maturation of human pluripotent stem cell derived cardiomyocytes in vitro – Correlation between contraction force and electrophysiology. *Biomaterials* **51**, 138–150 (2015).

59. Chan, Y. C. *et al.* Electrical stimulation promotes maturation of cardiomyocytes derived from human embryonic stem cells. *Journal of Cardiovascular Translational Research* **6**, 989–999 (2013).

60. Lemoine, M. D. *et al.* Human iPSC-derived cardiomyocytes cultured in 3D engineered heart tissue show physiological upstroke velocity and sodium current density. *Scientific reports* **7**, (2017).

61. Veldhuizen, J., Cutts, J., Brafman, D. A., Migrino, R. Q. & Nikkhah, M. Engineering anisotropic human stem cell-derived three-dimensional cardiac tissue on-a-chip. *Biomaterials* **256**, (2020).

62. Ribeiro, A. J. S. *et al.* Contractility of Single cardiomyocytes differentiated from pluripotent stem cells depends on physiological shape and substrate stiffness. *Proceedings of the National Academy of Sciences of the United States of America* **112**, 12705–12710 (2015).

63. Sun, N. *et al.* Patient-specific induced pluripotent stem cells as a model for familial dilated cardiomyopathy. *Science Translational Medicine* **4**, (2012).

64. Carvajal-Vergara, X. *et al.* Patient-specific induced pluripotent stem-cell-derived models of LEOPARD syndrome. *Nature* **465**, 808–812 (2010).

65. Zhang, M. *et al.* Recessive cardiac phenotypes in induced pluripotent stem cell models of Jervell and Lange-Nielsen syndrome: disease mechanisms and pharmacological rescue. *Proceedings of the National Academy of Sciences of the United States of America* **111**, E5383–E5392 (2014).

66. Burridge, P. W. *et al.* Human induced pluripotent stem cell-derived cardiomyocytes recapitulate the predilection of breast cancer patients to doxorubicin-induced cardiotoxicity. *Nature medicine* **22**, 547–556 (2016).

67. Klimas, A. *et al.* OptoDyCE as an automated system for high-throughput all-optical dynamic cardiac electrophysiology. *Nature communications* **7**, (2016).

68. di Pasquale, E. *et al.* CaMKII inhibition rectifies arrhythmic phenotype in a patient-specific model of catecholaminergic polymorphic ventricular tachycardia. *Cell death & disease* **4**, (2013).

69. Matsa, E. *et al.* Drug evaluation in cardiomyocytes derived from human induced pluripotent stem cells carrying a long QT syndrome type 2 mutation. *European heart journal* **32**, 952–962 (2011).

70. Milani-Nejad, N. & Janssen, P. M. L. Small and large animal models in cardiac contraction research: advantages and disadvantages. *Pharmacology & therapeutics* **141**, 235–249 (2014).

71. Mummery, C. L. *et al.* New Methods in Cardiovascular Biology MUSCLEMOTION A Versatile Open Software Tool to Quantify Cardiomyocyte and Cardiac Muscle Contraction In Vitro and In Vivo. (2017) doi:10.1161/CIRCRESAHA.

72. Kornreich, B. G. The patch clamp technique: Principles and technical considerations. *Journal of Veterinary Cardiology* **9**, 25–37 (2007).

73. Brown, A. P. Y. & Greenberg, H. Z. E. Patch clamp. *British journal of hospital medicine (London, England : 2005)* **77**, C74–C77 (2016).

74. Stett, A. *et al.* Biological application of microelectrode arrays in drug discovery and basic research. *Analytical and Bioanalytical Chemistry* **377**, 486–495 (2003).

75. Zanin, S., Lidron, E., Rizzuto, R. & Pallafacchina, G. Methods to measure intracellular Ca2+ concentration using Ca2+-sensitive dyes. in *Methods in Molecular Biology* vol. 1925 43–58 (Humana Press Inc., 2019).

76. van Meer, B. J., Tertoolen, L. G. J. & Mummery, C. L. Concise Review: Measuring Physiological Responses of Human Pluripotent Stem Cell Derived Cardiomyocytes to Drugs and Disease. *Stem Cells* **34**, 2008–2015 (2016).

77. Kitaguchi, T. *et al.* CSAHi study: Evaluation of multi-electrode array in combination with human iPS cell-derived cardiomyocytes to predict drug-induced QT prolongation and arrhythmia--effects of 7 reference compounds at 10 facilities. *Journal of pharmacological and toxicological methods* **78**, 93–102 (2016).

78. Hwang, H. S. *et al.* Comparable Calcium Handling Of Human iPSC-derived Cardiomyocytes Generated By Multiple Laboratories. *Journal of molecular and cellular cardiology* **85**, 79 (2015).

79. Passier, R., Orlova, V. & Mummery, C. Complex Tissue and Disease Modeling using hiPSCs. *Cell stem cell* **18**, 309–321 (2016).

80. Yang, X. & Papoian, T. Moving beyond the comprehensive in vitro proarrhythmia assay: Use of human-induced pluripotent stem cell-derived cardiomyocytes to assess contractile effects associated with drug-induced structural cardiotoxicity. *Journal of Applied Toxicology* **38**, 1166–1176 (2018).

81. Wang, J. H. C. & Lin, J. S. Cell traction force and measurement methods. *Biomechanics and Modeling in Mechanobiology* **6**, 361–371 (2007).

82. Hossain, M. M. *et al.* Non-invasive characterization of mouse embryonic stem cell derived cardiomyocytes based on the intensity variation in digital beating video. *The Analyst* **135**, 1624–1630 (2010).

83. Stummann, T. C. *et al.* Digital movie analysis for quantification of beating frequencies, chronotropic effects, and beating areas in cardiomyocyte cultures. *Assay and drug development technologies* **6**, 375–385 (2008).

84. Mukherjee, R., Crawford, F. A., Hewett, K. W. & Spinale, F. G. Cell and sarcomere contractile performance from the same cardiocyte using video microscopy. *Journal of applied physiology (Bethesda, Md. : 1985)* **74**, 2023–2033 (1993).

85. Goulart, J. T., Bassani, R. A. & Bassani, J. W. M. Application based on the Canny edge detection algorithm for recording contractions of isolated cardiac myocytes. *Computers in Biology and Medicine* **81**, 106–110 (2017).

86. Bazan, C., Barba, D. T., Blomgren, P. & Paolini, P. Image processing techniques for assessing contractility in isolated adult cardiac myocytes. *International journal of biomedical imaging* **2009**, (2009).

87. He, J. Q., Ma, Y., Lee, Y., Thomson, J. A. & Kamp, T. J. Human embryonic stem cells develop into multiple types of cardiac myocytes: Action potential characterization. *Circulation Research* **93**, 32–39 (2003).

88. Hayakawa, T. *et al.* Image-based evaluation of contraction-relaxation kinetics of human-induced pluripotent stem cell-derived cardiomyocytes: Correlation and complementarity with extracellular electrophysiology. *Journal of Molecular and Cellular Cardiology* **77**, 178–191 (2014).

89. Sala, L. *et al.* Musclemotion: A versatile open software tool to quantify cardiomyocyte and cardiac muscle contraction in vitro and in vivo. *Circulation Research* **122**, e5–e16 (2018).

90. Gesmundo, I. *et al.* Growth hormone-releasing hormone attenuates cardiac hypertrophy and improves heart function in pressure overload-induced heart failure. *Proceedings of the National Academy of Sciences of the United States of America* **114**, 12033–12038 (2017).

91. Shrivastava, S. & Schneider, M. F. Evidence for two-dimensional solitary sound waves in a lipid controlled interface and its implications for biological signalling. *Journal of the Royal Society, Interface* **11**, (2014).

92. el Hady, A. & Machta, B. B. Mechanical surface waves accompany action potential propagation. *Nature Communications 2015 6:1* **6**, 1–7 (2015).

93. Poznanski, R. R. *et al.* Solitonic conduction of electrotonic signals in neuronal branchlets with polarized microstructure. *Scientific reports* **7**, (2017).

94. Ozsoy, C., Ozbek, A., Reiss, M., Dean-Ben, X. L. & Razansky, D. Ultrafast four-dimensional imaging of cardiac mechanical wave propagation with sparse optoacoustic sensing. *Proceedings of the National Academy of Sciences of the United States of America* **118**, (2021).

95. Lagonegro, P. *et al.* Synthetic recovery of impulse propagation in myocardial infarction via silicon carbide semiconductive nanowires. *Nature communications* **13**, 6 (2022).

96. Xie, Y. *et al.* Effects of Fibroblast-Myocyte Coupling on Cardiac Conduction and Vulnerability to Reentry: A Computational Study. *Heart rhythm : the official journal of the Heart Rhythm Society* **6**, 1641 (2009).